

The effects of weak disorders on Quantum Hall critical points

Jinwu Ye

Department of Physics and Astronomy, The Johns Hopkins University, Baltimore MD, 21218
(May 10, 2018)

We study the consequences of random mass, random scalar potential and random vector potential on the line of fixed points between integer/fractional quantum Hall states and an insulator. This line of fixed points was first identified in a clean Dirac fermion system with both Chern-Simon coupling and Coulomb interaction in Phys. Rev. Lett. **80**, 5409 (1998). By performing a Renormalization Group analysis in $1/N$ (N is the No. of species of Dirac fermions) and the variances of three disorders $\Delta_M, \Delta_V, \Delta_A$, we find that Δ_M is irrelevant along this line, both Δ_A and Δ_V are marginal. With the presence of all the three disorders, the pure fixed line is unstable. Setting Chern-Simon interaction to zero, we find one non-trivial lines of fixed points in (Δ_A, w) plane with dynamic exponent $z = 1$ and continuously changing ν , it is *stable* against small (Δ_M, Δ_V) in a small range of the line $1 < w < 1.31$, therefore it may be relevant to integer quantum Hall transition. Setting $\Delta_M = 0$, we find a fixed plane with $z = 1$, the part of this plane with $\nu > 1$ is stable against small Δ_M , therefore it may be relevant to fractional quantum Hall transition. Although we do not find a generic fixed point with all the couplings *non-vanishing*, we prove that the theory is *renormalizable* to the order $(1/N)^2, (1/N)\Delta, \Delta^2$ and explore the interesting processes which describe the interferences between Chern-Simon interaction, Coulomb interaction and the three kinds of disorders.

I. INTRODUCTION

The zero temperature quantum phase transitions between the different quantum Hall and insulating states of a two-dimensional electron gas in a strong magnetic field are among the most intensively studied quantum critical points, both theoretically^{1,2} and experimentally³. Earlier theoretical investigations focussed on the transitions between the Integer Quantum Hall plateaus and described them in terms of non-interacting electrons moving in a random external potential⁴.

Ludwig *et al.* introduced and analyzed a Dirac fermion model with random mass, random scalar potential and random gauge potential. They found that the random mass is marginally *irrelevant*, random scalar potential marginally *relevant*. However, they found that random vector potential is exactly *marginal*, therefore there is a line of fixed points characterized by the strength of the random gauge potential, the zero energy wavefunction shows multifractal behaviors with the exponents continuously changing along the line⁵. If two of the random potentials are non-zero, the third one will be generated and the system flows to strong coupling regime. They further argued that the system should flow to the generic fixed point of integer Quantum Hall transitions which was correctly described by Chalker-Coddington model^{6,7}.

The properties of the fixed line of Dirac fermions in the presence of random magnetic fields were further investigated in Ref.^{8,9}. Later, the $U(1)$ gauge potential was extended to non-Abelian gauge potential¹⁰⁻¹².

It has also been argued that the transitions between fractional quantum Hall states could be mapped onto models essentially equivalent to those between the integer states¹³. The latter point of view was however questioned by Wen and Wu¹⁴ and Chen, Fisher and Wu¹⁵: they focussed on the simpler case of systems in the presence of a *periodic* rather than a random potential, and examined a model of anyons, with a statistical angle θ and short-range repulsive interactions, which displayed a second order quantum phase transition between a quantized Hall state and a Mott insulator as the strength of the periodic potential was varied. This transition was characterized by a line of critical points with continuously varying exponents, parameterized by the value of θ . For the case $\theta = 0$, when the anyons were fermions, the transition was out of a integer quantum Hall state; its exponents and other universal properties were different from the cases $0 < \theta < 2\pi$ for which the anyons acquired fractional statistics and the transition was out a fractional quantum Hall state. (For $\theta = 2\pi$ the anyons became bosons and the Hall state reduced to a superfluid.)

In all of the above theoretical works, the long-range Coulomb interactions between charge carriers have been effectively ignored. However, a few recent works have taken steps to remedy this serious shortcoming. Yang *et al.*¹⁶ studied the integer quantum Hall transition under a Hartree-Fock treatment of the Coulomb interaction. Lee and Wang¹⁷ showed that the renormalization group eigenvalue of the Coulomb interaction was zero at the Hartree-Fock critical point; higher order calculations are therefore necessary to understand the physics. Pfannkuche and MacDonald¹⁸ numerically studied electrons with Coulomb interactions in a periodic potential between a fractional

Hall state and an insulator, but were limited to rather small system sizes. Interesting scaling interpretations of Coulomb interaction-induced dephasing were discussed in Ref¹⁹.

Most recently, neglecting the disorders, Ye and Sachdev provided a thorough analysis of the consequences of Coulomb interactions on the anyons in a periodic potential model of Refs^{14,15}. They showed that the Coulomb interaction is *marginally irrelevant* for the integer case ($\theta = 0$), and remains so for the fractional case for small values of θ ; this marginally irrelevant interaction will lead to logarithmic corrections to naive scaling functions for the vicinity of the transition. For larger θ , they established, in a certain $1/N$ expansion, the existence of a novel line of fixed points at which the Coulomb interactions acquire a non-zero fixed point value determined by the value of θ . There are no logarithmic corrections at these fixed points, and naive scaling holds. They found a dynamic critical exponent $z = 1$ at all points on the fixed line, providing a concrete realization of the scenario^{23,2}, not previously established explicitly, that energies must scale as inverse distances for the $1/r$ Coulomb interaction. They also found the correlation length exponent $\nu > 2/d$ (where d is the spatial dimensionality) along this fixed line, which implies that the fixed line is stable against weak random mass disorder.

In this paper, we study in detail the consequences of random mass, random scalar potential and random vector potential at the line of fixed points. In the rest of this section, we introduce the notations and the model. In the next section, we give very general Renormalization Group (RG0 formulation of the model and establish some *exact* results (for example, Eqs.5 and 8). In Sec.III, we perform one-loop expansion and discuss the implications of R.G. flow equations. In Sec.IV, we first discuss the R.G. equation at $N = \infty$ limit, then calculate $1/N$ corrections and discuss the solutions in different cases. Finally, we reach conclusions in Sec. V. In the appendix, we show the equivalence of the two forms of the random vector gauge potential.

We begin our analysis by writing down the model of Ref²⁰ extended to include random mass $M(x)$, random scalar potential $V(x)$ and random vector potential $A_i(x)$ ⁵.

$$\begin{aligned} \mathcal{S} = & \int d^d x d\tau \left[\alpha \bar{\psi}_m \gamma_0 \partial_0 \psi_m + \bar{\psi}_m \gamma_i \partial_i \psi_m - \frac{i}{\sqrt{N}} q \mu^{\epsilon/2} \alpha^{1/2} a_0 \bar{\psi}_m \gamma_0 \psi_m - \frac{i}{\sqrt{N}} g \mu^{\epsilon/2} \alpha^{1/2} a_i \bar{\psi}_m \gamma_i \psi_m \right] \\ & + \int \frac{d^2 k d\omega}{4\pi^2 2\pi} \left[i k a_0(-\vec{k}, -\omega) a_t(\vec{k}, \omega) + \frac{k}{2} a_t(-\vec{k}, -\omega) a_t(\vec{k}, \omega) \right] \\ & + \int d^d x d\tau \left[i M(x) \bar{\psi}_m \psi_m + V(x) \bar{\psi}_m \gamma_0 \psi_m + i A_i(x) \bar{\psi}_m \gamma_i \psi_m \right] \end{aligned} \quad (1)$$

The ψ_m are $m = 1 \cdots N$ species of charge q/\sqrt{N} 2+1 dimensional Dirac fermions which interact with a $U(1)$ gauge field (a_0, a_i) ($i = 1, 2$); we are interested in the case $N = 1$ but will find the large N expansion to be a useful tool. The γ_0, γ_i are the Dirac γ matrices, $x_i(\tau)$ are spatial (temporal) co-ordinates with $\partial_0 \equiv \partial_\tau$, $\partial_i \equiv \partial_{x_i}$, and \vec{k}, ω ($k = |\vec{k}|$) are the Fourier transformed wavevector and frequency variables. To aid the subsequent renormalization group analysis, we are working in $d = 2 + \epsilon$ spatial dimensions and μ is a renormalization scale. The parameter α is introduced to allow for anisotropic renormalization between space and time²⁵. We have used the Coulomb gauge which allows us to explicitly represent a_i in terms of the transverse spatial component with $a_i = i \epsilon_{ij} k_j a_t / k$. The $a_0 a_t$ term in \mathcal{S} is the Chern Simons coupling: it turns the Dirac particles into anyons with a statistical angle θ/N with $\theta \equiv qg$; notice that the angle is of order $1/N$ and so the expected periodicity of the physics under $\theta/N \rightarrow \theta/N + 4\pi$ will not be visible in the $1/N$ expansion. The $a_t a_t$ term is the Coulomb interaction, and it has been written in terms of a_t following Ref²⁶.

In the absence of the Coulomb interaction and the random potential terms, it was shown in Ref¹⁵ that \mathcal{S} represents the critical theory of a system of anyons in a periodic potential undergoing a transition from an insulator with conductivities $\sigma_{xx} = \sigma_{xy} = 0$ into a fractional quantum Hall state with $\sigma_{xx} = 0$ and $\sigma_{xy} = (q^2/h)/(1 - \theta/2\pi)$ to leading order in $1/N$. Both these states have energy gaps. It was shown in Ref.²⁰ that the Coulomb interaction and disorder do not modify the values of σ_{ij} in either phase.

The relationship of the continuum model \mathcal{S} to the more realistic model of electrons studied in Ref¹⁸ remains somewhat unclear, although it is plausible that \mathcal{S} is the critical theory of the latter. We may also view \mathcal{S} as the simplest theory consistent with the following requirements, and therefore worthy of further study: (i) the two phases on either side of the critical point have the correct values of σ_{ij} , and the Hall phase has *both* quasi-particle and quasi-hole excitations with the correct charge and statistics, and (ii) the gap towards the quasi-particle *and* the quasi-hole excitations vanishes at the critical point.

II. THE RENORMALIZATION GROUP FORMULATION OF THE MODEL

We now proceed with a renormalization group analysis of \mathcal{S} . Simple power counting shows that the Chern-Simons, Coulomb interactions²² and all three kinds of disorders are marginal at tree level in $d = 2$, and so loop expansions are required and useful. Power counting also shows that a short-range four-fermion interaction term is *irrelevant* and has therefore been neglected in \mathcal{S} ; this makes the fermionic formulation of the anyon problem much simpler than its bosonic counterpart^{14,27,21}.

We assume all the three kinds of disorder satisfy Gaussian distribution with zero mean and variances $\Delta_M, \Delta_V, \Delta_A$.

$$\begin{aligned} \langle M(x)M(x') \rangle &= \Delta_M \delta^d(x - x') \\ \langle V(x)V(x') \rangle &= \Delta_V \delta^d(x - x') \\ \langle A_i(x)A_j(x') \rangle &= \delta_{ij} \Delta_A \delta^d(x - x') \end{aligned} \quad (2)$$

By introducing replica $a, b = 1, 2, \dots, n$ and doing quenched average over the above Gaussian distributions, we get

$$\begin{aligned} \mathcal{S} = & \int d^d x d\tau \left[\alpha \bar{\psi}_m^a \gamma_0 \partial_0 \psi_m^a + \bar{\psi}_m^a \gamma_i \partial_i \psi_m^a - \frac{i}{\sqrt{N}} q \mu^{\epsilon/2} \alpha^{1/2} a_0^a \bar{\psi}_m^a \gamma_0 \psi_m^a - \frac{i}{\sqrt{N}} g \mu^{\epsilon/2} \alpha^{1/2} a_i^a \bar{\psi}_m^a \gamma_i \psi_m^a \right] \\ & + \int \frac{d^2 k d\omega}{4\pi^2 2\pi} \left[i k a_0^a(-\vec{k}, -\omega) a_t^a(\vec{k}, \omega) + \frac{k}{2} a_t^a(-\vec{k}, -\omega) a_t^a(\vec{k}, \omega) \right] \\ & + \int d^d x d\tau d\tau' \left[\Delta_M \mu^\epsilon [\bar{\psi}_m^a(x, \tau) \psi_m^a(x, \tau)] [\bar{\psi}_m^b(x, \tau') \psi_m^b(x, \tau')] - \Delta_V \mu^\epsilon [\bar{\psi}_m^a(x, \tau) \gamma_0 \psi_m^a(x, \tau)] [\bar{\psi}_m^b(x, \tau') \gamma_0 \psi_m^b(x, \tau')] \right. \\ & \left. + \Delta_A \mu^\epsilon [\bar{\psi}_m^a(x, \tau) \gamma_i \psi_m^a(x, \tau)] [\bar{\psi}_m^b(x, \tau') \gamma_i \psi_m^b(x, \tau')] \right] \end{aligned} \quad (3)$$

The loop expansion requires counterterms to account for ultraviolet divergences in momentum integrals; we write the counter terms as

$$\begin{aligned} \mathcal{S}_{CT} = & \int d^d x d\tau \left[\alpha (Z_\alpha - 1) \bar{\psi}_m^a \gamma_0 \partial_0 \psi_m^a + (Z_2 - 1) \bar{\psi}_m^a \gamma_i \partial_i \psi_m^a \right. \\ & \left. - \frac{i}{\sqrt{N}} (Z_1^q - 1) q \mu^{\epsilon/2} \alpha^{1/2} a_0^a \bar{\psi}_m^a \gamma_0 \psi_m^a - \frac{i}{\sqrt{N}} (Z_1^g - 1) g \mu^{\epsilon/2} \alpha^{1/2} a_i^a \bar{\psi}_m^a \gamma_i \psi_m^a \right] \\ & + \int d^d x d\tau d\tau' \left[(Z_M - 1) \Delta_M \mu^\epsilon [\bar{\psi}_m^a(x, \tau) \psi_m^a(x, \tau)] [\bar{\psi}_m^b(x, \tau') \psi_m^b(x, \tau')] \right. \\ & \left. - (Z_V - 1) \Delta_V \mu^\epsilon [\bar{\psi}_m^a(x, \tau) \gamma_0 \psi_m^a(x, \tau)] [\bar{\psi}_m^b(x, \tau') \gamma_0 \psi_m^b(x, \tau')] \right. \\ & \left. + (Z_A - 1) \Delta_A \mu^\epsilon [\bar{\psi}_m^a(x, \tau) \gamma_i \psi_m^a(x, \tau)] [\bar{\psi}_m^b(x, \tau') \gamma_i \psi_m^b(x, \tau')] \right] \end{aligned} \quad (4)$$

In general, counter terms for the last two gauge field terms in \mathcal{S} should also be considered. However, it was shown²⁰ that at least to two loops, there no divergences associated with these terms. The Ward identities following from gauge invariance dictate

$$Z_1^q = Z_\alpha, \quad Z_1^g = Z_2 \quad (5)$$

Using these identities, we relate the bare fields and couplings in \mathcal{S} to the renormalized quantities by

$$\begin{aligned} \psi_{mB} &= Z_2^{1/2} \psi_m \\ \alpha_B &= (Z_\alpha / Z_2) \alpha \\ q_B &= q \mu^{\epsilon/2} (Z_\alpha / Z_2)^{1/2} \\ g_B &= g \mu^{\epsilon/2} (Z_2 / Z_\alpha)^{1/2} \\ \Delta_{MB} &= \mu^\epsilon \Delta_M Z_M / Z_2^2 \\ \Delta_{VB} &= \mu^\epsilon \Delta_V Z_V / Z_2^2 \\ \Delta_{AB} &= \mu^\epsilon \Delta_A Z_A / Z_2^2 \end{aligned} \quad (6)$$

Notice that these relations imply that for the statistical angle $\theta/N = qg/N$ we have $\theta_B = \theta\mu^\epsilon$ even in the presence of the Coulomb interaction and the disorders; so in $d = 2$ this angle is a renormalization group invariant, which is expected on general physical grounds.

The dynamic critical exponent, z is related to the renormalization of α by²⁵

$$z = 1 - \mu \frac{d}{d\mu} \ln \alpha = 1 - \mu \frac{d}{d\mu} \ln \frac{Z_2}{Z_\alpha} \quad (7)$$

We will find it convenient to express the loop expansion in terms of the ‘‘fine structure’’ constant $w \equiv q^2/16$, and a central object of study shall be its β -function $\beta(w) = \mu(dw/d\mu)$. By comparing (7) with relationships between bare and renormalized quantities quoted above we see that

$$z = 1 - \beta(w)/w. \quad (8)$$

Finally, the critical exponent ν is related to the anomalous dimension of the composite operator $\bar{\psi}\psi$ by $\nu^{-1} - 1 = \mu(d \ln Z_{\bar{\psi}\psi}/d\mu)$; the renormalization constant $Z_{\bar{\psi}\psi}$ can be calculated by inserting the operator into the self-energy diagrams.

III. ONE-LOOP CALCULATION

We begin the explicit calculation of the renormalization constants by considering a direct perturbative expansion in the Coulomb fine structure constant w , the statistical angle θ and the three kinds of disorders $\Delta_M, \Delta_V, \Delta_A$. At one-loop order (Fig.13, Fig.4a,b,c), we find no dependence on θ ; the values of the renormalization constants upto terms of order $w^2, \theta^2, w\theta$ and Δ^2 are

$$\begin{aligned} Z_2 &= 1 - 2w/N\pi\epsilon \\ Z_\alpha &= 1 - \frac{1}{\pi\epsilon}(\Delta_M + \Delta_V + 2\Delta_A) \end{aligned} \quad (9)$$

We also explicitly verified that the Ward identities Eq.5 hold.

From Fig.5-Fig.10 and Fig.13a-d, we can calculate the three renormalization constants for the disorders (the details are given in the next section where we perform a similar calculations in large N limit):

$$\begin{aligned} Z_M &= 1 + \frac{1}{\pi\epsilon\Delta_M}(2\Delta_M^2 + 2\Delta_M\Delta_V - 4\Delta_M\Delta_A - 4\Delta_V\Delta_A) - \frac{8w}{N\pi\epsilon} \\ Z_V &= 1 - \frac{2}{\pi\epsilon\Delta_V}(\Delta_M\Delta_V + 2\Delta_M\Delta_A + \Delta_V\Delta_V + 2\Delta_V\Delta_A) \\ Z_A &= 1 - \frac{2}{\pi\epsilon\Delta_A}\Delta_M\Delta_V - \frac{4w}{N\pi\epsilon} \end{aligned} \quad (10)$$

From Eq.6, we obtain the four β functions:

$$\begin{aligned} \beta(w) &= \beta^p(w) - \frac{w}{\pi}(\Delta_M + \Delta_V + 2\Delta_A) \\ \beta(\Delta_M) &= -2\Delta_M(\nu_p^{-1} - 1) + \frac{2}{\pi}(\Delta_M^2 + \Delta_M\Delta_V - 2\Delta_M\Delta_A - 2\Delta_V\Delta_A) \\ \beta(\Delta_V) &= 2\Delta_V \frac{\beta^p(w)}{w} - \frac{2}{\pi}(\Delta_M\Delta_V + 2\Delta_M\Delta_A + \Delta_V^2 + 2\Delta_V\Delta_A) \\ \beta(\Delta_A) &= -\frac{2}{\pi}\Delta_M\Delta_V \end{aligned} \quad (11)$$

Where the β -function of the Coulomb coupling in the *pure* system $\beta^p(w)$ is²⁰:

$$\beta^p(w) = \frac{2w^2}{N\pi} + \mathcal{O}(w^3, w^2\theta^2) \quad (12)$$

While the *pure* critical exponent ν_p is²⁰:

$$\nu_p = 1 - 2w/N\pi \quad (13)$$

From Eq.11, we can identify the *disordered* critical exponent ν :

$$\nu^{-1} = \nu_p^{-1} - \frac{\Delta_M}{\pi} - \frac{\Delta_V}{\pi} + \frac{2\Delta_A}{\pi} \quad (14)$$

From the first and the third equations in Eq.11, we find $\beta(\Delta_V)$ and $\beta(w)$ are related by

$$\beta(\Delta_V) = 2\Delta_V \frac{\beta(w)}{w} - \frac{4}{\pi} \Delta_M \Delta_A \quad (15)$$

In Eq.11, setting Coulomb interaction and two of the random potentials to be zero, we reproduce the results of Ludwig *et.al*⁵.

With the presence of Coulomb interaction $w \neq 0$, we discuss the three cases separately:

$\Delta_M \neq 0$

The system flows to a line of *stable* fixed points given by $\Delta_M = \frac{2w}{N}$. The flow trajectory is given by $\Delta_M = \frac{C}{w^2}$, C is an arbitrary constant(Fig.16a). From Eqs.13, 14, we find $\nu = 1$ along this line, it saturates the bound $\nu \geq 2/d$ (d is the special dimension).

$\Delta_V \neq 0$

There exists a line of *unstable* fixed points given by $\Delta_V = \frac{2w}{N}$. The flow trajectory is given by $\Delta_V = Cw^2$ (Fig.16b). Below this line, the system flows to the origin, above this line, the system flows to strong coupling regime. From Eqs.13, 14, we find $\nu = 1$ along this line.

$\Delta_A \neq 0$

The system flows to a line of *stable* fixed points given by $\Delta_A = \frac{w}{N}$. The flow trajectory is given by $\Delta_A = C$ (Fig.16c). From Eqs.13, 14, we find $\nu = 1 - \frac{4\Delta_A}{\pi}$ which continuously changes along this line. It should be noted that $\nu < 1$ along this line.

From Eq.8, it is easy to see that $z = 1$ on all these line of fixed points. It is also worth noting that, despite the value $z = 1$, the critical correlators are *not* Lorentz invariant.

In the generic case, we do not find any perturbative accessible *stable* fixed point. The system flows to the strong coupling regime. In the next section, we resort to the large N expansion to explore the strong coupling regime.

IV. LARGE N EXPANSION

To understand larger values of θ , and to explore the consequences of a possible interference between the Coulomb interactions, disorders and the Chern-Simons term we found it convenient to perform a $1/N$ expansion. This is technically simpler than a perturbative two-loop extension of the computation of the last section and also automatically includes the dynamic screening of the gauge field propagator by the fermion polarization²⁶. Alternatively stated, the so-called RPA approximation becomes exact at $N = \infty$, and $1/N$ corrections require gauge field propagators which have the RPA form

$$\mathcal{S}_{RPA} = \frac{1}{2} \int \frac{d^2k}{4\pi^2} \frac{d\omega}{2\pi} (a_0, a_t) \begin{pmatrix} q^2 k^2 / (16\sqrt{k^2 + \omega^2}) & ik \\ ik & k + g^2 / (16\sqrt{k^2 + \omega^2}) \end{pmatrix} \begin{pmatrix} a_0 \\ a_t \end{pmatrix} \quad (16)$$

The inverse of the above matrix leads to the propagators of the gauge fields:

$$\begin{aligned} G_{00}(q, \nu) &= \frac{1}{q^2} \frac{q + \frac{q^2}{16} \sqrt{q^2 + \nu^2}}{1 + (\frac{\theta}{16})^2 + \frac{e^2}{16} \frac{q}{\sqrt{q^2 + \nu^2}}} \\ G_{0i}(q, \nu) &= \frac{\epsilon_{ij} q_j}{q^2} \frac{1}{1 + (\frac{\theta}{16})^2 + \frac{e^2}{16} \frac{q}{\sqrt{q^2 + \nu^2}}} \\ G_{0i}(q, \nu) &= -G_{i0}(q, \nu) \\ G_{ij}(q, \nu) &= (\delta_{ij} - \frac{q_i q_j}{q^2}) \frac{e^2/16}{[1 + (\frac{\theta}{16})^2] \sqrt{q^2 + \nu^2} + \frac{e^2}{16} q} \end{aligned} \quad (17)$$

To the order of $(\frac{1}{N})^0 \Delta$, the summation of Fig.1 (a),(b),(c),(d),(e) leads to *effective* random scalar potential $\tilde{\Delta}_V$:

$$\tilde{\Delta}_V = \frac{\Delta_V + \Delta_A \phi}{(\lambda + w)^2} \quad (18)$$

where $\phi \equiv (\theta/16)^2$ and $\lambda = 1 + \phi$.

Note that both Δ_V and Δ_A contribute to the effective random scalar potential with the *same* sign.

To the order of $(\frac{1}{N})^0 \Delta$, the summation of Fig.2 (a),(b),(c),(d),(e) leads to *effective* random vector potential $\tilde{\Delta}_A(\delta_{ij} - \frac{q_i q_j}{q^2})$ (see the appendix):

$$\tilde{\Delta}_A = \frac{\Delta_V \phi + \Delta_A(1+w)^2}{(\lambda+w)^2} \quad (19)$$

Note that both Δ_A and Δ_V contribute to the effective random vector potential with the *same* sign.

To the order of $(\frac{1}{N})^0 \Delta$, the summation of Fig.3 (a),(b),(c),(d) leads to *effective* random Scalar-Vector potential $\tilde{\Delta}_C \frac{\epsilon_{ij} q_j}{q}$:

$$\tilde{\Delta}_C = \frac{2\sqrt{\phi}}{(\lambda+w)^2} [-\Delta_V + \Delta_A(1+w)] \quad (20)$$

It should be noted that both Δ_A and Δ_V contribute to the effective random SV potential with the *opposite* sign and there is *no* such random SV potential in the original action Eq.3. Due to the interference between disorder and CS interaction, this potential is generated. But it can only appear as *internal* lines. Putting $\phi = 0$ (namely, no CS interaction), this potential vanishes.

These three effective potentials plus the random mass potential and the four RPA gauge fields propagators in Eq.17 are the building blocks in the following Feymann diagrams. Note that, however, only *bare* disorder potentials can appear as *external* lines of any Feymann diagram.

In the following, we discuss $N = \infty$ case first, then we discuss $1/N$ correction. It is well known that only *primitive* divergences of Feymann diagrams are needed in the RG flow equation.

A. $N = \infty$ limit

Fig.4 is the contributions to the Dirac fermion self-energy from the effective random potentials. The divergent parts from the effective random SV potentials (d) and (e) vanish. We find the two constants defined in Eq.4:

$$\begin{aligned} Z_2 &= 1 \\ Z_\alpha &= 1 - \frac{1}{\pi\epsilon} (\Delta_M + \tilde{\Delta}_V + 2\tilde{\Delta}_A) \end{aligned} \quad (21)$$

In the following, the notation $A \rightarrow B$ means that A renormalizes B .

Fig.5 is the renormalization from the random mass (In this figure and the following figures, we do not draw explicitly the diagrams with the exchange of leg3 and leg 4).

$$\begin{aligned} 5a = -5b &= \frac{\Delta_M^2}{\pi\epsilon} \rightarrow \Delta_A \\ 5c = 5d &= \frac{2\Delta_M^2}{\pi\epsilon} \rightarrow \Delta_M \end{aligned} \quad (22)$$

In all, Fig.5 contributes $\frac{4\Delta_M^2}{\pi\epsilon} \rightarrow \Delta_M$.

Fig.6 is the renormalization from the interference of random mass and *effective* random scalar potential. Note the effective random scalar potential can only appear in the *internal loops*.

$$\begin{aligned} 6a = 6b = 6c = 6d &= -\frac{\Delta_M \tilde{\Delta}_V}{\pi\epsilon} \rightarrow \Delta_A \\ 6e = 6f &= \frac{2\Delta_M \tilde{\Delta}_V}{\pi\epsilon} \rightarrow \Delta_M \\ 6g = 6h &= \frac{2\Delta_M \Delta_V}{\pi\epsilon} \rightarrow \Delta_V \end{aligned} \quad (23)$$

In all, Fig.6 contributes $\frac{4\Delta_M \tilde{\Delta}_V}{\pi\epsilon} \rightarrow \Delta_M$, $\frac{4\Delta_M \Delta_V}{\pi\epsilon} \rightarrow \Delta_V$, $-\frac{4\Delta_M \tilde{\Delta}_V}{\pi\epsilon} \rightarrow \Delta_A$

Fig.7 is the renormalization from the interference of random mass and *effective* random vector potential.

$$\begin{aligned}
7a=7b &= \frac{2\Delta_M\tilde{\Delta}_A}{\pi\epsilon} \rightarrow \Delta_M, \frac{2\Delta_M\tilde{\Delta}_A}{\pi\epsilon} \rightarrow \Delta_V \\
7c=7d &= -\frac{2\Delta_M\tilde{\Delta}_A}{\pi\epsilon} \rightarrow \Delta_M, \frac{2\Delta_M\tilde{\Delta}_A}{\pi\epsilon} \rightarrow \Delta_V \\
7e=7f &= -\frac{4\Delta_M\tilde{\Delta}_A}{\pi\epsilon} \rightarrow \Delta_M \\
7g=7h &= 0
\end{aligned} \tag{24}$$

In all, Fig.7 contributes $-\frac{8\Delta_M\tilde{\Delta}_A}{\pi\epsilon} \rightarrow \Delta_M, \frac{8\Delta_M\tilde{\Delta}_A}{\pi\epsilon} \rightarrow \Delta_V$.

Fig.8 is the renormalization from the random scalar potential.

$$\begin{aligned}
8a=-8b &= \frac{\tilde{\Delta}_V^2}{\pi\epsilon} \rightarrow \Delta_A \\
8c=8d &= \frac{2\Delta_V\tilde{\Delta}_V}{\pi\epsilon} \rightarrow \Delta_V
\end{aligned} \tag{25}$$

In all, Fig.8 contributes $\frac{4\Delta_V\tilde{\Delta}_V}{\pi\epsilon} \rightarrow \Delta_V$.

Fig.9 is the renormalization from the interference of effective random scalar potential and effective random vector potential.

$$\begin{aligned}
9a=9b &= -\frac{2\tilde{\Delta}_V\tilde{\Delta}_A}{\pi\epsilon} \rightarrow \Delta_M, -\frac{2\tilde{\Delta}_V\tilde{\Delta}_A}{\pi\epsilon} \rightarrow \Delta_V \\
9c=9d &= -\frac{2\tilde{\Delta}_V\tilde{\Delta}_A}{\pi\epsilon} \rightarrow \Delta_M, \frac{2\tilde{\Delta}_V\tilde{\Delta}_A}{\pi\epsilon} \rightarrow \Delta_V \\
9e=9f &= \frac{4\Delta_V\tilde{\Delta}_A}{\pi\epsilon} \rightarrow \Delta_V \\
9g=9h &= 0
\end{aligned} \tag{26}$$

In all, Fig.9 contributes $-\frac{8\tilde{\Delta}_V\tilde{\Delta}_A}{\pi\epsilon} \rightarrow \Delta_M, \frac{8\Delta_V\tilde{\Delta}_A}{\pi\epsilon} \rightarrow \Delta_V$.

Fig.10 is the renormalization from the effective random vector potential.

$$\begin{aligned}
10a=-10b &= \frac{4\tilde{\Delta}_A^2}{\pi\epsilon} \rightarrow \Delta_A \\
10c=10d &= 0
\end{aligned} \tag{27}$$

In all, Fig.10 does *not* contribute.

Fig.11 is the renormalization from the effective random SV potential.

$$\begin{aligned}
11a=11d=-11e=-11h &= -\frac{\tilde{\Delta}_C^2}{4\pi\epsilon} \rightarrow \Delta_A \\
11b=11c=11f=11g &= -\frac{\tilde{\Delta}_C^2}{2\pi\epsilon} \rightarrow \Delta_M
\end{aligned} \tag{28}$$

In all, Fig.11 contributes $-\frac{2\tilde{\Delta}_C^2}{\pi\epsilon} \rightarrow \Delta_M$. It can be shown that only when SV potential get paired, there are *non-zero* contributions.

Fig.12 is the renormalization to the random mass from random effective scalar, vector and scalar-vector potentials.

$$\begin{aligned}
12a=12h &= \frac{16\Delta_M\tilde{\Delta}_A}{\pi\epsilon} \frac{w+\phi}{\lambda+w} \rightarrow \Delta_M \\
12b=12c=12f=12g &= \frac{8\Delta_M\tilde{\Delta}_C}{\pi\epsilon} \frac{\sqrt{\phi}}{\lambda+w} \rightarrow \Delta_M \\
12d=12e &= -\frac{16\Delta_M\tilde{\Delta}_V}{\pi\epsilon} \frac{\phi}{\lambda+w} \rightarrow \Delta_M
\end{aligned} \tag{29}$$

In all, Fig.12 contributes $-\frac{32\Delta_M}{\pi\epsilon} \frac{1}{\lambda+w} [\phi\tilde{\Delta}_V - (w+\phi)\tilde{\Delta}_A - \sqrt{\phi}\tilde{\Delta}_C] \rightarrow \Delta_M$.

From Fig5-Fig.12, we find the three constants Z_M, Z_V, Z_A defined in Eq.4:

$$\begin{aligned}
Z_M &= 1 + \frac{1}{\pi\epsilon\Delta_M}(2\Delta_M^2 + 2\Delta_M\tilde{\Delta}_V - 4\Delta_M\tilde{\Delta}_A - 4\tilde{\Delta}_V\tilde{\Delta}_A - \tilde{\Delta}_C^2 - 16\Delta_M\tilde{\Delta}_K) \\
Z_V &= 1 - \frac{2}{\pi\epsilon\Delta_V}(\Delta_M\Delta_V + 2\Delta_M\tilde{\Delta}_A + \Delta_V\tilde{\Delta}_V + 2\Delta_V\tilde{\Delta}_A) \\
Z_A &= 1 - \frac{2}{\pi\epsilon\Delta_A}\Delta_M\tilde{\Delta}_V
\end{aligned} \tag{30}$$

Where $\tilde{\Delta}_K$ is given by

$$\tilde{\Delta}_K = \frac{\Delta_V\phi(3-w-\phi) + \Delta_A[\phi^2 - (w+\phi)(1+w)^2 - 2\phi(1+w)]}{(\lambda+w)^3} \tag{31}$$

From Eq.6, we can find the following β functions at $N = \infty$.

$$\begin{aligned}
\beta(w) &= -\frac{w}{\pi}(\Delta_M + P(\tilde{\Delta}_V) + 2P(\tilde{\Delta}_A)) \\
\beta(\Delta_M) &= \frac{2}{\pi}\Delta_M^2 + \frac{1}{\pi}\tilde{\Delta}_C^2 + \frac{4}{\pi}\tilde{\Delta}_V\tilde{\Delta}_A + \frac{2}{\pi}(\Delta_M - 2\tilde{\Delta}_A)P(\tilde{\Delta}_V) - \frac{4}{\pi}(\Delta_M + \tilde{\Delta}_V)P(\tilde{\Delta}_A) \\
&\quad - \frac{2}{\pi}\tilde{\Delta}_C P(\tilde{\Delta}_C) - \frac{16}{\pi}\Delta_M P(\tilde{\Delta}_K) \\
\beta(\Delta_V) &= -\frac{2}{\pi}\Delta_M\Delta_V - \frac{2}{\pi}\Delta_V P(\tilde{\Delta}_V) - \frac{4}{\pi}(\Delta_M + \Delta_V)P(\tilde{\Delta}_A) \\
\beta(\Delta_A) &= -\frac{2}{\pi}\Delta_M P(\tilde{\Delta}_V)
\end{aligned} \tag{32}$$

Where the function $P(\Delta) = \Delta_V \frac{\partial \Delta}{\partial \Delta_V} + \Delta_A \frac{\partial \Delta}{\partial \Delta_A} + w \frac{\partial \Delta}{\partial w} + 2\phi \frac{\partial \Delta}{\partial \phi}$.

We shall discuss the implications of this equation after considering $1/N$ corrections in the next subsection.

B. $1/N$ correction

In this section, we consider $1/N$ correction to $N = \infty$ results. The small parameters are $1/N, \Delta_M, \Delta_V, \Delta_A$. We expect that if there are fixed points, the fixed points values of Δ^{ts} are of the order $1/N$.

Fig.13 is the contribution to the Dirac fermion self energy from $1/N$ fluctuation of gauge fields given by Eq.17. Actually, Fig.13b and Fig.13c are convergent. The results are²⁰

$$\begin{aligned}
Z_2 &= 1 - \frac{\Psi_A}{N\pi\epsilon} = 1 - \frac{1}{N\pi\epsilon} \left(\frac{2w}{\lambda} - \frac{16w^2A}{\pi\lambda} + \frac{\theta^2C}{16\pi} - \frac{\theta^2E}{16\pi} \right) \\
Z_\alpha &= 1 - \frac{\Psi_V}{N\pi\epsilon} = 1 - \frac{1}{N\pi\epsilon} \left(\frac{16w^2B}{\pi\lambda} - \frac{\theta^2D}{16\pi} + \frac{\theta^2F}{16\pi} \right),
\end{aligned} \tag{33}$$

where $\lambda = 1 + (\theta/16)^2$ and the functions $A, B, C, D, E = A + B, F = B$ are given by the formal expressions

$$\begin{aligned}
A &= \int_0^1 dx \frac{4x^2(1-x^2)}{(1+x^2)^3} f(x; w, \theta), & B &= \int_0^1 dx \frac{(1-x^2)(1-6x^2+x^4)}{(1+x^2)^3} f(x; w, \theta) \\
C &= \int_0^1 dx \frac{4x^2}{(1-x^2)(1+x^2)} f(x; w, \theta), & D &= \int_0^1 dx \frac{(1-6x^2+x^4)}{(1-x^2)(1+x^2)} f(x; w, \theta)
\end{aligned} \tag{34}$$

with $f(x; w, \theta) = (\lambda(1+x^2) + w(1-x^2))^{-1}$, and the variable x represents an intermediate frequency. Note the two constants C, D are divergent: this divergence is due to the singular effect of frequencies $|\omega| \gg k$. However, as shown in Ref²⁰, these divergences are gauge artifacts and cancel in the β -function and in any physical gauge-invariant quantity like ν, z or σ_{ij} . The divergences however do infect the anomalous dimension of the field operator ψ : this is as expected as the propagator of ψ is clearly gauge-dependent.

Fig.14 is the renormalization to Δ_M from the $1/N$ fluctuation of gauge fields. Actually, Fig.14b and Fig.14c are convergent, the divergent parts are

$$\frac{\Psi_M}{N\pi\epsilon} = \frac{1}{N\pi\epsilon} \left[\frac{4w}{\lambda} \left(1 - \frac{4w(2A+B)}{\pi} \right) + \frac{\theta^2(2C+D)}{16\pi} + \frac{\theta^2(2A+B)}{16\pi} - \frac{\theta^2 G}{2\pi} \right] \quad (35)$$

Where the function G is given by

$$G = \int_0^1 dx [(\phi-1)(1-x^2) + w \frac{(1-x^2)^2}{1+x^2}] f^2(x; w, \theta) \quad (36)$$

It is easy to see Fig.14 is exactly *the same* diagram for the calculation of $Z_{\bar{\psi}\psi}$ as expected²⁰, therefore $Z_2 Z_{\bar{\psi}\psi} = 1 - \Psi_M/N\pi\epsilon$.

In Fig14, replacing Δ_M line by Δ_V and Δ_A lines, we can repeat the same calculation. In fact, the divergent parts should be $\frac{\Psi_V}{N\pi\epsilon}$ and $\frac{\Psi_A}{N\pi\epsilon}$ respectively as dictated by Ward identities. It can be shown explicitly that Fig.15a + Fig15b vanishes as dictated by Ward Identities.

Adding the $1/N$ correction to the renormalization constants calculated in the last section, we obtain

$$\begin{aligned} Z_2 &= 1 - \frac{\Psi_A}{N\pi\epsilon} \\ Z_\alpha &= 1 - \frac{1}{\pi\epsilon} (\Delta_M + \tilde{\Delta}_V + 2\tilde{\Delta}_A) - \frac{\Psi_V}{N\pi\epsilon} \\ Z_M &= 1 + \frac{1}{\pi\epsilon\Delta_M} (2\Delta_M^2 + 2\Delta_M\tilde{\Delta}_V - 4\Delta_M\tilde{\Delta}_A - 4\tilde{\Delta}_V\tilde{\Delta}_A - \tilde{\Delta}_C^2 - 16\Delta_M\tilde{\Delta}_K) - \frac{2\Psi_M}{N\pi\epsilon} \\ Z_V &= 1 - \frac{2}{\pi\epsilon\Delta_V} (\Delta_M\Delta_V + 2\Delta_M\tilde{\Delta}_A + \Delta_V\tilde{\Delta}_V + 2\Delta_V\tilde{\Delta}_A) - \frac{2\Psi_V}{N\pi\epsilon} \\ Z_A &= 1 - \frac{2}{\pi\epsilon\Delta_A} \Delta_M\tilde{\Delta}_V - \frac{2\Psi_A}{N\pi\epsilon} \end{aligned} \quad (37)$$

From Eq.6, we can find $1/N$ corrections to the β functions in Eq.32.

$$\begin{aligned} \beta(w) &= \beta^p(w) - \frac{w}{\pi} (\Delta_M + P(\tilde{\Delta}_V) + 2P(\tilde{\Delta}_A)) \\ \beta(\Delta_M) &= -2\Delta_M(\nu_p^{-1} - 1) + \frac{2}{\pi}\Delta_M^2 + \frac{1}{\pi}\tilde{\Delta}_C^2 + \frac{4}{\pi}\tilde{\Delta}_V\tilde{\Delta}_A + \frac{2}{\pi}(\Delta_M - 2\tilde{\Delta}_A)P(\tilde{\Delta}_V) \\ &\quad - \frac{4}{\pi}(\Delta_M + \tilde{\Delta}_V)P(\tilde{\Delta}_A) - \frac{2}{\pi}\tilde{\Delta}_C P(\tilde{\Delta}_C) - \frac{16}{\pi}\Delta_M P(\tilde{\Delta}_K) \\ \beta(\Delta_V) &= 2\Delta_V \frac{\beta^p(w)}{w} - \frac{2}{\pi}\Delta_M\Delta_V - \frac{2}{\pi}\Delta_V P(\tilde{\Delta}_V) - \frac{4}{\pi}(\Delta_M + \Delta_V)P(\tilde{\Delta}_A) \\ \beta(\Delta_A) &= -\frac{2}{\pi}\Delta_M P(\tilde{\Delta}_V) \end{aligned} \quad (38)$$

The $\beta^p(w)$ in Eq.38 is the β -function of the Coulomb coupling in the *pure* case which was calculated in Ref.²⁰:

$$\begin{aligned} \beta^p(w) &= \frac{2w^2(1-\phi)}{N\pi^2\lambda^2} \left[\pi - 16w \int_0^1 dx \left(\frac{1-x^2}{1+x^2} \right)^3 \frac{\lambda(1+x^2) + \frac{w}{2}(1-x^2)}{(\lambda(1+x^2) + w(1-x^2))^2} \right] \\ &\quad + \frac{32w\phi}{N\pi^2} \int_0^1 dx \frac{(1-x^2)(-1+10x^2-x^4)}{(1+x^2)^3} \frac{(1+x^2) + \frac{w}{2}(1-x^2)}{(\lambda(1+x^2) + w(1-x^2))^2}, \end{aligned} \quad (39)$$

The *pure* exponent ν_p in Eq.38 is given by

$$\begin{aligned} \nu_p^{-1} - 1 &= \frac{2w(1-\phi)}{N\pi^2\lambda^2} \left[\pi - 16w \int_0^1 dx \left(\frac{1-x^2}{1+x^2} \right)^3 \frac{\lambda(1+x^2) + \frac{w}{2}(1-x^2)}{(\lambda(1+x^2) + w(1-x^2))^2} \right] \\ &\quad + \frac{32\phi}{N\pi^2} \int_0^1 dx \left(\frac{1-x^2}{1+x^2} \right)^3 \frac{1+x^2 + \frac{w}{2}(1-x^2)}{(\lambda(1+x^2) + w(1-x^2))^2} \\ &\quad - \frac{192\phi}{N\pi^2} \int_0^1 dx \left(\frac{1-x^2}{1+x^2} \right) \frac{1+x^2 + \frac{w}{2}(1-x^2)}{(\lambda(1+x^2) + w(1-x^2))^2} \\ &\quad + \frac{512\phi(1-\phi)}{N\pi^2} \int_0^1 dx \frac{(1-x^2)(1+x^2)}{(\lambda(1+x^2) + w(1-x^2))^3} \end{aligned} \quad (40)$$

The explicit expressions for $P^{i's}$ are given by

$$\begin{aligned}
P(\tilde{\Delta}_V) &= \frac{1}{(\lambda+w)^3} [\Delta_V(1-w-3\phi) + \Delta_A\phi(3+w-\phi)] \\
P(\tilde{\Delta}_A) &= \frac{1}{(\lambda+w)^3} [\Delta_V\phi(3+w-\phi) + \Delta_A(1+w)[(1+w)^2 - (3+w)\phi]] \\
P(\tilde{\Delta}_C) &= \frac{2\sqrt{\phi}}{(\lambda+w)^3} [-2\Delta_V(1-\phi) + \Delta_A[(\lambda+w)w + 2(1+w)(1-\phi)]] \\
P(\tilde{\Delta}_K) &= \frac{1}{(\lambda+w)^3} \{ \Delta_V\phi(9-4w-5\phi) + \Delta_A[5\phi^2 - (1+w)^2(2w+3\phi) - 6\phi(1+w) - 2w(w+\phi)(1+w) - 2\phi w] \} \\
&\quad - \frac{3(w+2\phi)}{(\lambda+w)^4} \{ \Delta_V\phi(3-w-\phi) + \Delta_A[\phi^2 - (w+\phi)(1+w)^2 - 2\phi(1+w)] \}
\end{aligned} \tag{41}$$

From the second equation in Eq.38, we can identify the *disordered* critical exponent

$$\nu^{-1} = \nu_p^{-1} - \frac{\Delta_M}{\pi} - \frac{P(\tilde{\Delta}_V)}{\pi} + \frac{2P(\tilde{\Delta}_A)}{\pi} + \frac{8P(\tilde{\Delta}_K)}{\pi} \tag{42}$$

At fixed points, substituting $\frac{\beta^p(w)}{w} = \frac{1}{\pi}(\Delta_M + P(\tilde{\Delta}_V) + 2P(\tilde{\Delta}_A))$ into Eq.40, we can simplify the above equation to

$$\nu^{-1} = \tilde{\nu}_p^{-1} + \frac{4P(\tilde{\Delta}_A)}{\pi} + \frac{8P(\tilde{\Delta}_K)}{\pi} \tag{43}$$

Where $\tilde{\nu}_p^{-1}$ is listed in Eq.12 of Ref.²⁰:

$$\begin{aligned}
\tilde{\nu}_p^{-1} - 1 &= -\frac{128\phi}{N\pi^2} \int_0^1 dx \frac{(1-x^2)(1+6x^2+x^4)}{(1+x^2)^3} \frac{1+x^2 + \frac{w}{2}(1-x^2)}{(\lambda(1+x^2) + w(1-x^2))^2} \\
&\quad + \frac{512\phi(1-\phi)}{N\pi^2} \int_0^1 dx \frac{(1-x^2)(1+x^2)}{(\lambda(1+x^2) + w(1-x^2))^3}
\end{aligned} \tag{44}$$

It can be checked that Eq.15 should be replaced by:

$$\beta(\Delta_V) = 2\Delta_V \frac{\beta(w)}{w} - \frac{4}{\pi} \Delta_M P(\tilde{\Delta}_A) \tag{45}$$

In Eq.38, we expand $\beta(w)$ to order $1/N$ and Δ , expand $\beta(\Delta)$ to $(1/N)\Delta, \Delta^2$. It is easy to see there should be *no* $(1/N)^2$ terms in $\beta(\Delta)$, because interactions do not generate disorder (or equivalently disorder do not generate interactions). Note that the small parameter $1/N$ plays a similar role to the small parameter ϵ in the conventional ϵ expansion, namely, we are trying to locate the fixed points at $\Delta^{i's}$ at the order of $1/N$.

We now turn to the physical implications of our main results (38), (39) and (40).

If there exists only random mass, namely, $\Delta_V = \Delta_A = 0$, Eq.38 simplifies to

$$\begin{aligned}
\beta(w) &= \beta^p(w) - \frac{w}{\pi} \Delta_M \\
\beta(\Delta_M) &= -2\Delta_M(\nu_p^{-1} - 1) + \frac{2}{\pi} \Delta_M^2 = -2\Delta_M(\tilde{\nu}_p^{-1} - 1)
\end{aligned} \tag{46}$$

Setting all the disorders vanishing, the authors in Ref.²⁰ found a line of *pure* fixed points given by $\beta^p(w) = 0$. They also found that $\tilde{\nu}_p > 1$ along the fixed line, therefore concluded that this line is stable against weak random mass disorder from Harris criterion. Here, we explicitly write down $\beta(\Delta_M)$ to the order $(1/N)\Delta_M, \Delta_M^2$ and reach a *stronger* statement that there are *no* other fixed points except this line in the weak coupling regime.

Comparing Eq.32 to Eq.38, we find that there is *no* $1/N$ correction to $\beta(\Delta_A)$, therefore Δ_A is always marginal. The $1/N$ correction to $\beta(\Delta_V)$ is simply $\beta^p(w)/w$, therefore Δ_V is marginal along this line, irrelevant(relevant) *above(below)* this line. Actually, these results are expected from Ward identities. We also find that $1/N$ correction to $\beta(\Delta_M)$ is just $\nu_p^{-1} - 1$, which is consistent with Harris criterion.

With the presence of all the three disorders, we expect that the *pure* fixed line is unstable.

1. Integer Quantum Hall Transition ($\phi = 0$)

First, considering the transition out of the integer quantum Hall state, $\theta = 0$, which implies $\phi = 0$, $\lambda = 1$. The $\beta^p(w)$ is simplified to²⁰

$$\frac{\beta^p(w)}{w} = \frac{2w}{N\pi^2} \left[\pi - 16w \int_0^1 dx \left(\frac{1-x^2}{1+x^2} \right)^3 \frac{1+x^2 + \frac{w}{2}(1-x^2)}{(1+x^2 + w(1-x^2))^2} \right] \quad (47)$$

Eq.40 reduces to $\nu_p^{-1} - 1 = \beta^p(w)/w$. The simple analysis of (39) shows that $\beta^p(w) > 0$ for all $w > 0$; for small w we have $\beta^p(w)/w = 2w/(N\pi)$, in agreement with one-loop result (12), while for $w \gg 1$, $\beta(w) = 4/(N\pi w)$. So the only *pure* fixed point remains at $w = 0$. The whole picture of $\beta^p(w)/w$ is drawn in Fig.17a,c, it increases linearly first, reaches a maximum value $0.20/N$ at $w = 1.31$ and eventually decays as $1/w$.

It is easy to see that $\tilde{\Delta}_V = \frac{\Delta_V}{(1+w)^2}$, $P(\tilde{\Delta}_V) = \Delta_V \frac{1-w}{(1+w)^3}$; $\tilde{\Delta}_A = P(\tilde{\Delta}_A) = \Delta_A$; $\tilde{\Delta}_C = P(\tilde{\Delta}_C) = 0$; $\tilde{\Delta}_K = -\Delta_A \frac{w}{1+w}$, $P(\tilde{\Delta}_K) = -\Delta_A \frac{w(w+2)}{(1+w)^2}$. Substituting these expressions into Eq.38. we find that Eq.38 is simplified to

$$\begin{aligned} \frac{\beta(w)}{w} &= \frac{\beta^p(w)}{w} - \frac{1}{\pi} (\Delta_M + \Delta_V \frac{1-w}{(1+w)^3} + 2\Delta_A) \\ \beta(\Delta_M) &= -2\Delta_M \frac{\beta^p(w)}{w} + \frac{2}{\pi} \Delta_M^2 + \frac{2}{\pi} (\Delta_M - 2\Delta_A) \Delta_V \frac{1-w}{(1+w)^3} + \frac{4}{\pi} \Delta_M \Delta_A (3 - \frac{4}{(1+w)^2}) \\ \beta(\Delta_V) &= 2\Delta_V \frac{\beta^p(w)}{w} - \frac{2}{\pi} \Delta_M \Delta_V - \frac{2}{\pi} \Delta_V^2 \frac{1-w}{(1+w)^3} - \frac{4}{\pi} (\Delta_M + \Delta_V) \Delta_A \\ \beta(\Delta_A) &= -\frac{2}{\pi} \Delta_M \Delta_V \frac{1-w}{(1+w)^3} \end{aligned} \quad (48)$$

Eq.42 is simplified to

$$\nu^{-1} = \nu_p^{-1} - \frac{\Delta_M}{\pi} - \frac{\Delta_V}{\pi} \frac{1-w}{(1+w)^3} + \frac{2\Delta_A}{\pi} - \frac{8\Delta_A}{\pi} \frac{w(w+2)}{(1+w)^2} \quad (49)$$

Eq.45 is simplified to

$$\beta(\Delta_V) = 2\Delta_V \frac{\beta(w)}{w} - \frac{4}{\pi} \Delta_M \Delta_A \quad (50)$$

We discuss the three cases separately:

$\Delta_M \neq 0$

The system flows to a line of *stable* fixed points given by $\Delta_M = \pi \frac{\beta^p(w)}{w}$. Like the one-loop result, $\nu = 1$ and the flow trajectory is given by $\Delta_M = \frac{C}{w^2}$, C is an arbitrary constant $\sim 1/N$ (Fig.17a). We suspect that $\nu = 1$ is *exact* (namely, independent of large N limit).

This line is *unstable* against small Δ_V and Δ_A .

$\Delta_V \neq 0$

There exists a line of fixed points given by $\Delta_V = \pi \frac{(1+w)^3}{1-w} \frac{\beta^p(w)}{w}$ which approaches ∞ as $w \rightarrow 1^-$. Like the one loop result, $\nu = 1$ and the flow trajectory is given by $\Delta_V = Cw^2$ (Fig.17b). Again, we suspect that $\nu = 1$ is *exact*.

The lower part of this line (thin part) is *unstable*, the higher part of this line (thick part) is *stable*. The system either flows to the origin or flows to the higher part depending on the initial condition.

This line is *unstable* against small Δ_M and Δ_A .

$\Delta_A \neq 0$

The system flows to a line of fixed points given by $\Delta_A = \frac{\pi}{2} \frac{\beta^p(w)}{w}$. Like one loop result, the flow trajectory is given by $\Delta_A = C$ (Fig.17c). However, *unlike* one loop result, $\nu^{-1} = 1 - \frac{4\Delta_A}{\pi} (1 - \frac{2}{(1+w)^2})$, if $w > \sqrt{2} - 1 \sim 0.41$, $\nu > 1$. The left part of this line (thick part) is *stable*, the right part of this line (thin part) is *unstable*. At weak disorder, the system either flows to the left part of the line or to strong coupling regime depending on the initial condition. At strong disorder, the system always flows to strong coupling regime.

This line is *stable* against small Δ_M and Δ_V in the range $1 < w < 1.31$. This stable region may control the integer quantum Hall transitions observed in real experimental systems¹.

As shown first by Ludwig *et al*⁵, the random gauge fixed line is unstable against Δ_M and Δ_V (see also Eq.11). Due to the Coulomb interaction, we find there is a small part of the fixed line $1 < w < 1.31$ which is *stable* against small Δ_M and Δ_V .

From Eq.8, it is easy to see that $z = 1$ on all these line of fixed points.

Unfortunately, we are still unable to find a generic fixed points with all the couplings *non-vanishing*. These generic fixed points may be either inaccessible to the method developed in this paper, or simply do not exist in the real experimental system.

2. Fractional Quantum Hall Transition ($\phi > 0$)

Turning to the fractional case with a non-zero θ , we start with the simplest case $w = \Delta_V = \Delta_A = 0$, $\beta(\Delta_M)$ simplifies to

$$\beta(\Delta_M) = -2\Delta_M(\nu_p^{-1} - 1) + \frac{2}{\pi}\Delta_M^2 \quad (51)$$

Where ν_p is the exponent in the absence of Coulomb interactions ($w = 0$):

$$\nu_p = 1 - \frac{512\phi(1-2\phi)}{N3\pi^2\lambda^3} \quad (52)$$

When $0 < \phi < 1/2$, $\nu_p < 1$, the pure fixed point is unstable, the system flows to a line of fixed points given by $\Delta_M = \frac{512\phi(1-2\phi)}{N3\pi\lambda^3}$. From Eq.8 and the fact $\frac{\beta^p(w)}{w}|_{w=0} = 0$, we obtain $z = 1 + \Delta_M/\pi > 1$ which continuously changes along this line (Fig.18). From Eq.42, we get $\nu = 1$ along this line. When $\phi > 1/2$, the pure line of fixed points with $z = 1$ is stable.

It is easy to see that this fixed line is unstable against small (w, Δ_V, Δ_A).

Unlike the Coulomb interaction case ($\theta = 0$), if $\Delta_V \neq 0$ or $\Delta_A \neq 0$, then all the three disorders are generated, this can be easily realized from Eq.38. So we have to investigate the generic fixed points of Eq.38.

From Eq.38, $\beta(\Delta_A) = 0$ implies either $P(\tilde{\Delta}_V) = 0$ or $\Delta_M = 0$. In the following, we discuss the two cases separately.

$P(\tilde{\Delta}_V) = 0$

From Eq.45 and Eq.38, $\beta(w) = \beta(\Delta_V) = 0$ implies that $P(\tilde{\Delta}_A) = 0$, $\beta^p(w)/w = \Delta_M/\pi$. Finally, $\beta(\Delta_M) = 0$ implies

$$-2\Delta_M(\tilde{\nu}_p^{-1} - 1) + \frac{1}{\pi}\tilde{\Delta}_C^2 + \frac{4}{\pi}\tilde{\Delta}_V\tilde{\Delta}_A - \frac{2}{\pi}\tilde{\Delta}_C P(\tilde{\Delta}_C) - \frac{16}{\pi}\Delta_M P(\tilde{\Delta}_K) = 0 \quad (53)$$

The *disordered* critical exponent Eq.43 is simplified to

$$\nu^{-1} = \tilde{\nu}_p^{-1} + \frac{8P(\tilde{\Delta}_K)}{\pi} \quad (54)$$

It is easy to see that $P(\tilde{\Delta}_V) = P(\tilde{\Delta}_A) = 0$ implies the following equation:

$$t = \frac{\Delta_V}{\Delta_A} = \frac{\phi(3+w-\phi)}{w+3\phi-1} = \frac{(1+w)[(3+w)\phi - (1+w)^2]}{\phi(3+w-\phi)} \quad (55)$$

Namely, $x = 1 + w$ should satisfy the *fourth* order equation:

$$x^4 + 2(\phi-1)x^3 - 2\phi^2x^2 - 2\phi(\phi-1)(\phi+2)x + \phi^2(2-\phi)^2 = 0 \quad (56)$$

with the constraints $3+w > \phi$, $\phi > \frac{1-w}{3}$, $\phi > \frac{(1+w)^2}{3+w}$.

From Ref.²⁰, $\beta^p(w)/w = \Delta_M/\pi > 0$ implies that $\phi < 2$, therefore $w < \sqrt{5}$.

If $\phi = 0$, Eq.56 reduces to $x^3(x-2) = 0$, therefore $w = 1$. If $0 < \phi < 1$, there is *no* real root which satisfies both $x > 1$ and the constraints.

If $\phi = 1$, Eq.56 reduces to $(x^2 - 1)^2 = 0$ which implies that $w = 0$. Substituting ($\phi = 1, w = 0, t = 1$) into Eq.41, we find $\tilde{\Delta}_C = P(\tilde{\Delta}_C) = P(\tilde{\Delta}_K) = 0$.

If $1 < \phi < 2$, there is only one real root with $x > 1$. We also find $P(\tilde{\Delta}_K) < 0$, therefore $\nu > \tilde{\nu}_p > 1$ in this regime.

Unfortunately, when substituting the (ϕ, w, t) into Eq.53, we find that the left hand side of the equation is always *positive*. Therefore, we conclude there is *no* perturbatively accessible fixed points with $\Delta_M, \Delta_V, \Delta_A > 0$.

$$\underline{\Delta_M = 0}$$

From Eq.45, we see that $\beta(w) = 0$ implies $\beta(\Delta_V) = 0$. From Eq.38, it leads to

$$\frac{\beta^p(w)}{w} = \frac{1}{\pi}(P(\tilde{\Delta}_V) + 2P(\tilde{\Delta}_A)) \quad (57)$$

From Eq.38, $\beta(\Delta_M) = 0$ leads to

$$\frac{1}{\pi}\tilde{\Delta}_C^2 + \frac{4}{\pi}\tilde{\Delta}_V\tilde{\Delta}_A - \frac{4}{\pi}\tilde{\Delta}_AP(\tilde{\Delta}_V) - \frac{4}{\pi}\tilde{\Delta}_VP(\tilde{\Delta}_A) - \frac{2}{\pi}\tilde{\Delta}_CP(\tilde{\Delta}_C) = 0 \quad (58)$$

From the last equation, given (ϕ, t) , we can determine w , then substituting (ϕ, w, t) to Eq.57, we can determine Δ_A, Δ_V . In the following, we consider the two end lines separately:

(a) $\Delta_V = 0$ (namely $t = 0$)

If $\phi = 0$, Eq.58 becomes an identity, we recover the results of the IQHT (Fig.17c).

If $\phi > 0$, the solution of Eq.58 is $w = \frac{1}{2}[3\phi + \sqrt{(3\phi)^2 + 4(1-\phi)} - 4] > 0$ (namely, $\phi > 3/5$). Substituting this expression into Eq.57, we can determine $\tilde{\Delta}_A$ and the constraint $\phi < 1.3$. Thus ϕ must satisfy $3/5 < \phi < 1.3$. From Eq.43, we find this line is stable against small Δ_M .

(b) $\Delta_A = 0$ (namely $t = \infty$)

If $\phi = 0$, Eq.58 becomes an identity, we recover the results of the IQHT (Fig.17b).

If $\phi > 0$, the solution of Eq.58 is $w = 3 - 5\phi$. Substituting $w = 3 - 5\phi$ into Eq.57, we can determine Δ_V : $\frac{\beta^p(w)}{w} = \frac{\Delta_V}{32\pi} \frac{6\phi-1}{(1-\phi)^2}$. Therefore ϕ must satisfy $1/6 < \phi < 3/5$. Eq.43 becomes $\nu^{-1} = \tilde{\nu}_p^{-1} + \frac{3\Delta_V}{8\pi} \frac{\phi^2}{(1-\phi)^3} > \tilde{\nu}_p^{-1} > 1$, therefore, this line is unstable against small Δ_M .

We conjecture that there is a fixed *plane* which connect the above two end lines at $t = 0$ and at $t = \infty$ (Fig.19). The shaded (unshaded) region has $\nu > 1$ ($\nu < 1$), therefore is stable (unstable) against small Δ_M . Numerical analysis is needed to determine its precise boundary. The stable region may control the fractional quantum hall transitions observed in real experimental systems².

V. CONCLUSION

Recent experiments indicated that the transitions between two Quantum Hall states or between a quantum Hall state and an insulating state may be described by quantum critical theories. In these theories, different FQH states and insulating states are considered as different ground states of the electron systems. The three important questions remain unsolved on the nature of these quantum phase transitions are:

- (a) The effects of the quasi-particle statistics
- (b) The effects of long-ranged Coulomb interaction on the transitions
- (c) The effects of all kinds of disorders

Answering the three questions at the same time seems a forbidding task at this moment. Ref.²⁰ investigated the combined effects of (a) and (b) in a Dirac fermion model and found a line of fixed points. Along this line, both Chern-Simon interaction and Coulomb interaction are non-vanishing, the dynamic exponent $z = 1$. In this paper, we make a serious attempt to study the combined effects of (a), (b) and (c) in the Dirac fermion model. We perform a renormalization Group analysis by the systematic perturbative expansions in $1/N$ (N is the No. of species of Dirac fermions) and the variances of three disorders $\Delta_M, \Delta_V, \Delta_A$. we find that Δ_M is irrelevant along this line; there is *no* $1/N$ correction to $\beta(\Delta_A)$, therefore Δ_A is always marginal; Δ_V is marginal along this line, , irrelevant *above* this line, relevant *below* this line. With the presence of all the three disorders, the pure fixed line is unstable.

In IQHT, in the three special cases, we find the three non-trivial lines of fixed points with dynamic exponent $z = 1$.

The fixed line in (Δ_M, w) plane has $\nu = 1$ and is unstable against small (Δ_V, Δ_M) .

The fixed line in (Δ_V, w) plane has $\nu = 1$ and is unstable against small (Δ_M, Δ_A) .

Most interestingly, the fixed line in (Δ_A, w) plane has continuously changing ν and is *stable* against small (Δ_M, Δ_V) in the small range $1 < w < 1.31$ (Fig.17), this stable region may control the integer quantum Hall transitions observed in real experimental systems¹.

The results may be relevant to the IQH to insulator transitions. It may also be important to high T_c superconductors. Because it was well-established that high T_c superconductors have a d-wave order parameter and its quasiparticle excitations are described by 2 + 1 dimensional Dirac fermions²⁴.

In FQHT, setting Coulomb interaction to zero and $\Delta_V = \Delta_A = 0$, we find a line of fixed points with $\nu = 1$ and $z > 1$ which continuously changes along this line (see Fig.18). This line is unstable against small (w, Δ_V, Δ_A) .

Most interestingly, setting $\Delta_M = 0$, we find a fixed plane with $z = 1$, the part of this plane with $\nu > 1$ is stable against small Δ_M . This stable region may control the fractional quantum Hall transitions observed in real experimental systems².

Unfortunately, we are unable to find a generic fixed points with all the couplings *non-vanishing*. These generic fixed points may be either inaccessible to the method developed in this paper, or simply do not exist in the real experimental system. However, by looking at carefully the divergent structures of all the relevant Feynmann diagrams, we show the model is *renormalizable* to the order $(1/N)\Delta, \Delta^2, (1/N)^2$ discussed in this paper; we do bring out the systematic and elegant structure which describes the interferences between Chern-Simon interaction, Coulomb interaction and the three kinds of disorders. We believe that the structure is interesting in its own right and may inspire future work to study this difficult problem.

Acknowledgments

We thank M. P. A. Fisher, B. Halperin, A. Millis, C. Mudry, S. Kivelson, N. Read, S. Sachdev and X. G. Wen for helpful discussions. This work was supported by NSF Grant No. DMR-97-07701.

- ¹ B. Huckenstein, Rev. Mod. Phys. **67**, 357 (1995).
- ² S. L. Sondhi, S. M. Girvin, J. P. Carini and D. Shahar, Rev. Mod. Phys. **69**, 315 (1997).
- ³ L.W. Engel, D. Shahar, C. Kurdak, and D.C. Tsui, Phys. Rev. Lett. **71**, 2638 (1993); H.P. Wei, L.W. Engel and D.C. Tsui, Phys. Rev. B **50**, 14609 (1994); D. Shahar, D.C. Tsui, M. Shayegan, E. Shimshoni and S.L. Sondhi, Science, **274**, 589 (1996).
- ⁴ A.M.M. Pruisken in *The Quantum Hall Effect*, R.E. Prange and S.M. Girvin eds, Springer-Verlag, New York (1990);
- ⁵ A. W. W. Ludwig, M.P.A. Fisher, R. Shankar and G. Grinstein, Phys. Rev. B **48**, 13749, (1993).
- ⁶ J. T. Chalker and P. D. Coddington, J. Phys. C **21**, 2665 (1988).
- ⁷ D. H. Lee, Z. Wang and S. Kivelson, Phys. Rev. Lett. **70**, 4130 (1993).
- ⁸ C. Chamon, C. Mudry, and X. G. Wen, Phys. Rev. Lett. **77**, 4194 (1996); H. E. Castillo *et al.* Phys. Rev. B **56**, 10668 (1997).
- ⁹ I. Kogan, C. Mudry and A. M. Tsvelik, Phys. Rev. Lett. **77**, 707 (1996).
- ¹⁰ C. Mudry, C. Chamon and X. G. Wen, Nucl. Phys. B **466**, 383 (1996); Phys. Rev. B **53**, R7638 (1996).
- ¹¹ J. S. Caux, N. Taniguchi and A. M. Tsvelik, Phys. Rev. Lett. **80**, 1276 (1998); cond-mat/9801055.
- ¹² C. Mudry, B. D. Simons and A. Altland, Phys. Rev. Lett. **80**, 4257 (1998).
- ¹³ J.K. Jain, S. Kivelson and N. Trivedi, Phys. Rev. Lett. **64**, 1297 (1990); S. Kivelson, D.H. Lee and S.C. Zhang, Phys. Rev. B **46**, 2223 (1992).
- ¹⁴ X.G. Wen and Y.S. Wu, Phys. Rev. Lett. **70**, 1501 (1993).
- ¹⁵ W. Chen, M.P.A. Fisher and Y.S. Wu, Phys. Rev. B **48**, 13749, (1993).
- ¹⁶ S.R. Eric Yang and A.H. MacDonald, Phys. Rev. Lett. **70**, 4110 (1993); S.R. Eric Yang, A.H. MacDonald and B. Huckenstein, *ibid* **74**, 3229 (1995).
- ¹⁷ D.-H. Lee and Z. Wang, Phys. Rev. Lett. **76**, 4014 (1996).
- ¹⁸ D. Pfannkuche and A.H. MacDonald, Phys. Rev. B **56**, R7100 (1997) .
- ¹⁹ D.G. Polyakov and K.V. Samokhin, report No. cond-mat/9705154.
- ²⁰ Jinwu Ye and S. Sachdev, Phys. Rev. Lett. **80**, 5409 (1998); J. Ye and S. Sachdev, unpublished.
- ²¹ Jinwu Ye, Phys. Rev. B **58**, 9450 (1998).
- ²² S. Sachdev, Phys. Rev. B **57**, 7157 (1998).
- ²³ M.P.A. Fisher, Phys. Rev. Lett. **65**, 923 (1990).
- ²⁴ T. Senthil, M.P. A. Fisher, L. Balents and C. Nayak, Phys. Rev. Lett. **81**, 4704 (1998).
- ²⁵ E. Brezin and J. Zinn-Justin, Phys. Rev. B **13**, 251 (1976); D. Boyanovsky and J. Cardy, *ibid*, **26**, 154 (1982).
- ²⁶ B.I. Halperin, P.A. Lee and N. Read, Phys. Rev. B **47**, 7312 (1993).
- ²⁷ M.P.A. Fisher and G. Grinstein, Phys. Rev. Lett. **60**, 208 (1988).
- ²⁸ For example, see the book by Ryder, Quantum Field Theory, Cambridge University Press (1985). See also the appendix of Ref.²¹.

APPENDIX A: THE PROOF OF EQUIVALENCE OF RANDOM VECTOR GAUGE POTENTIAL $\Delta_A \delta_{IJ}$ AND $\Delta_A (\delta_{IJ} - \frac{Q_I Q_J}{Q^2})$.

We can decompose the random gauge field $A_i(x)$ in Eq.1 into transverse and longitudinal components:

$$A_i = A_i^T + A_i^L = \epsilon_{ij} \partial_j \chi^T + \partial_i \chi^L \quad (\text{A1})$$

Where $\chi^T(x), \chi^L(x)$ satisfy

$$\langle \chi^T(x)\chi^T(x') \rangle = \langle \chi^L(x)\chi^L(x') \rangle = -\Delta_A \ln|x-x'| \quad (\text{A2})$$

From the above equation, it can be shown easily

$$\begin{aligned} \langle A_i^T(k)A_j^T(k') \rangle &= \Delta_A(\delta_{ij} - \frac{k_i k_j}{k^2}), \\ \langle A_i^L(k)A_j^L(k') \rangle &= \Delta_A \frac{k_i k_j}{k^2} \end{aligned} \quad (\text{A3})$$

Adding the two equations above leads to

$$\langle A_i(x)A_j(x') \rangle = \langle A_i^T(x)A_j^T(x') \rangle + \langle A_i^L(x)A_j^L(x') \rangle = \Delta_A \delta_{ij} \delta^d(x-x') \quad (\text{A4})$$

which is the third equation of Eq.2.

By gauge transformation, $A_i^L(x) = \partial_i \chi^L(x)$ can be removed, so $\langle A_i^L(k)A_j^L(k') \rangle = \Delta_A \frac{k_i k_j}{k^2}$ should *not* make any contribution to *gauge-invariant* quantities. This fact is similar to the "running gauge fixing parameter" in usual relativistic quantum field theory²⁸. This point can also be demonstrated in the following specific example.

Let us evaluate its contribution to fermion self energy Fig.4c, the divergent part is

$$\frac{1}{2\pi\epsilon}(\gamma_0\omega + \gamma_i k_i) \quad (\text{A5})$$

It is evident that although this contribution infect the anomalous dimension of the field operator ψ , it does not affect the dynamic exponent z which is a gauge invariant quantity.

Figure Captions

FIG. 1. The effective random scalar potential $\tilde{\Delta}_V$ to the order $(1/N)^0 \Delta_V$ and $(1/N)^0 \Delta_A$. The thick dashed line is the effective random scalar potential. The thin dashed lines are the bare random scalar and vector potentials. The wave line is the gauge fields propagators.

FIG. 2. The effective random vector potential $\tilde{\Delta}_A$ to the order $(1/N)^0 \Delta_A$ and $(1/N)^0 \Delta_V$. The thick dashed line is the effective random vector potential. The thin dashed lines are the bare random scalar and vector potentials.

FIG. 3. The effective random Scalar-Vector potential $\tilde{\Delta}_C$ to the order $(1/N)^0 \Delta_A$ and $(1/N)^0 \Delta_V$. The thick dashed line is the effective random SV potential. There is *no* bare random SV potential.

FIG. 4. The contribution to the Dirac fermion self-energy from random potentials.

FIG. 5. The renormalization from the random mass.

FIG. 6. The renormalization from the interference of random mass and *effective* random scalar potential. Note the effective random scalar potential can only appear in the *internal loops*

FIG. 7. The renormalization from the interference of random mass and *effective* random vector potential

FIG. 8. The renormalization from the random scalar potential

FIG. 9. The renormalization from the interference of effective random scalar potential and effective random vector potential

FIG. 10. The renormalization from the effective random vector potential

FIG. 11. The renormalization from the effective random SV potential

FIG. 12. The Renormalization to random mass from $\tilde{\Delta}_V, \tilde{\Delta}_A, \tilde{\Delta}_C$. In the text, it is called $\tilde{\Delta}_K$. Compare this figure to Fig.13.

FIG. 13. The renormalization to the Dirac fermion self-energy from gauge fields fluctuations to order $1/N$

FIG. 14. The renormalization to the random mass from gauge fields fluctuation to the order $1/N$

FIG. 15. The fermion bubbles which contribute to the renormalization of random scalar and vector potentials. In the figure, $\mu, \nu, \lambda = 0, 1, 2$.

FIG. 16. The One-Loop Renormalization Group flow of (a) random mass and Coulomb interaction (b) random scalar potential and Coulomb interaction (c) random gauge potential and Coulomb interaction

FIG. 17. The Renormalization Group flow to order $1/N$ of (a) random mass and Coulomb interaction (b) random scalar potential and Coulomb interaction (c) random gauge potential and Coulomb interaction. The thick (thin) lines in (b) and (c) are *stable(unstable)* line of fixed points.

FIG. 18. The Renormalization Group flow to order $1/N$ of random mass and Chern-Simon interaction

FIG. 19. If $\Delta_M = 0$, there is a fixed plane in $(\phi, t = \Delta_V/\Delta_A)$ plane. w and Δ_A and Δ_V are uniquely determined by (ϕ, t) , therefore are not shown in the figure. The shaded regime with $z = 1, \nu > 1$ is stable against small Δ_M .

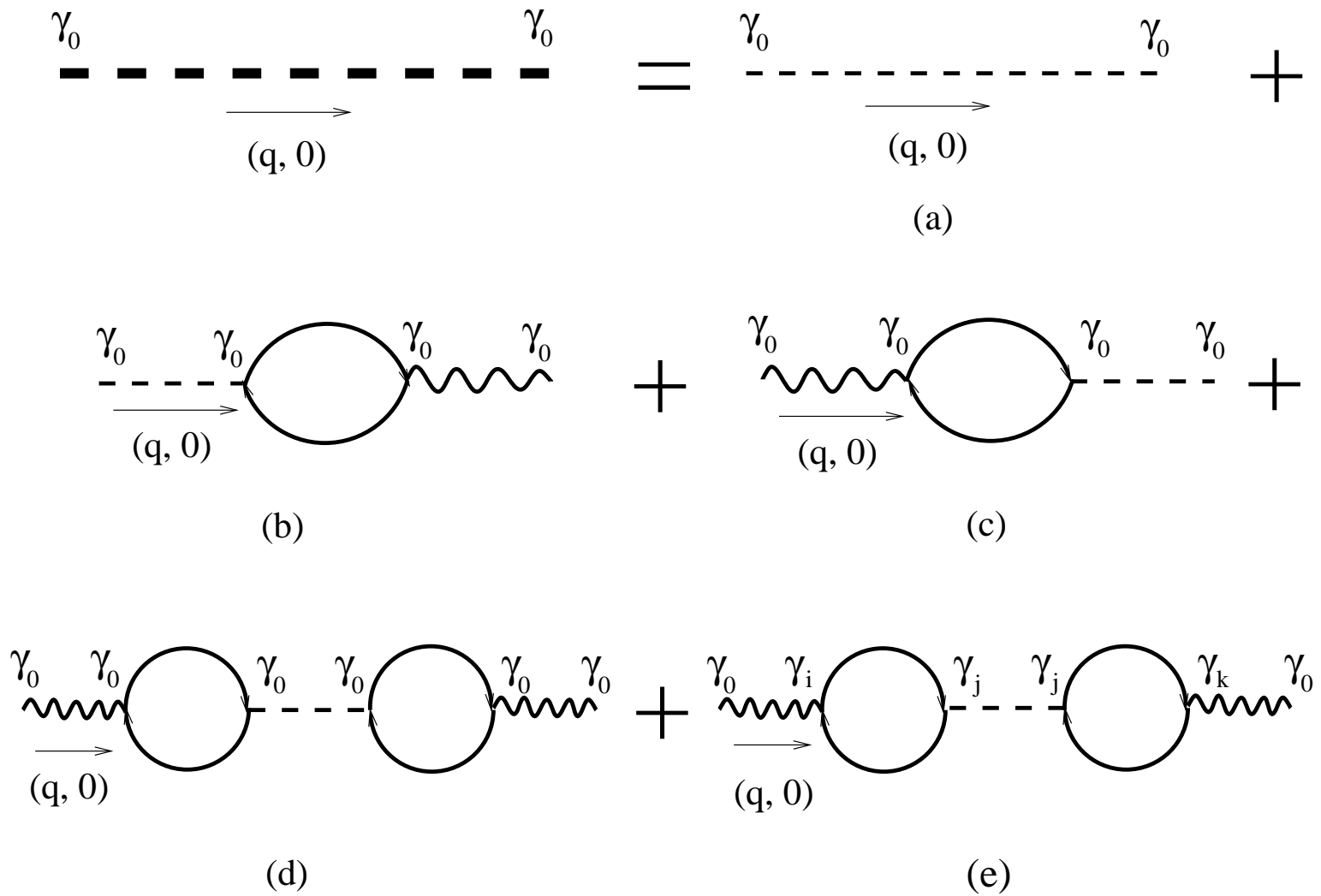


Fig.1

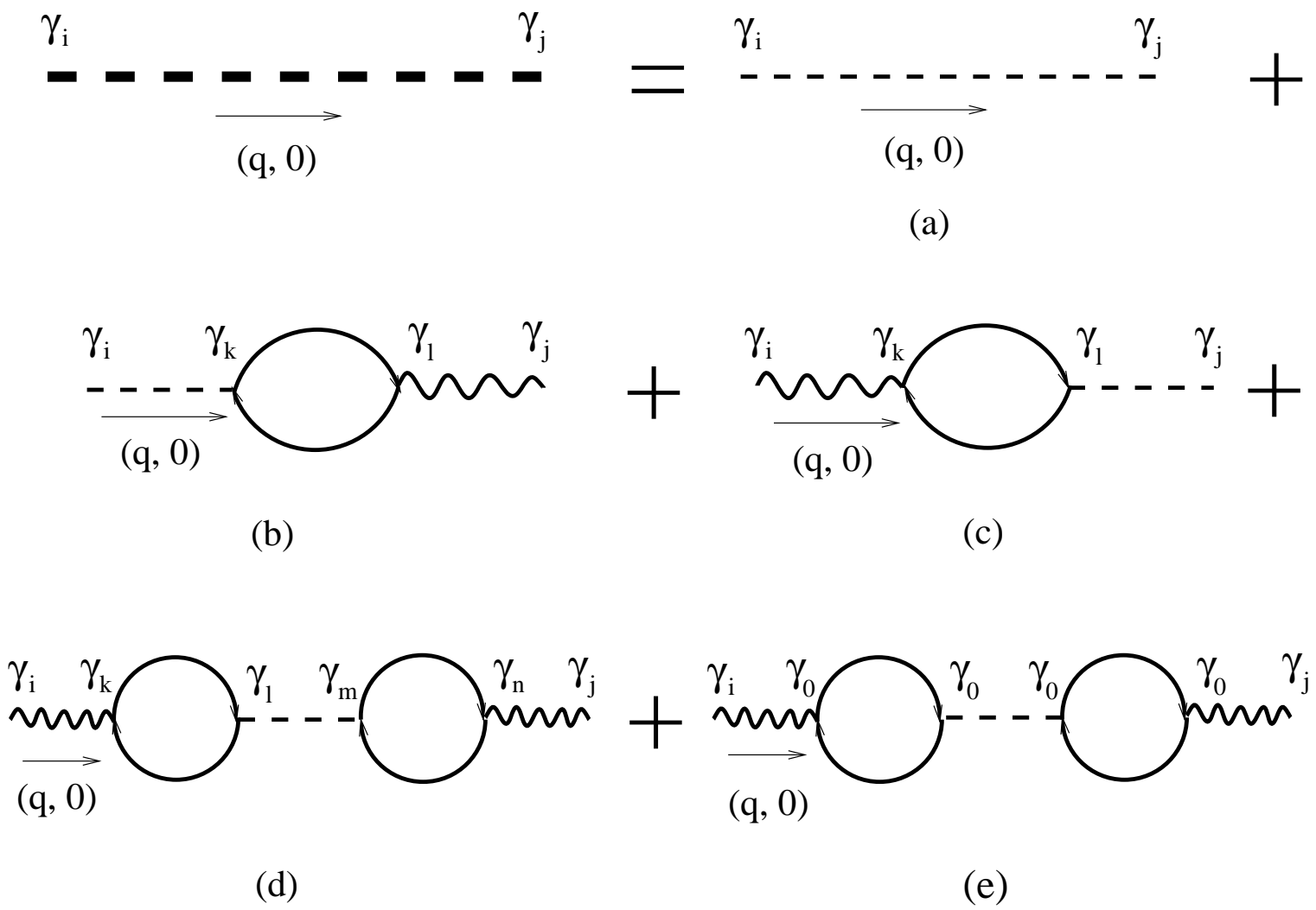


Fig.2

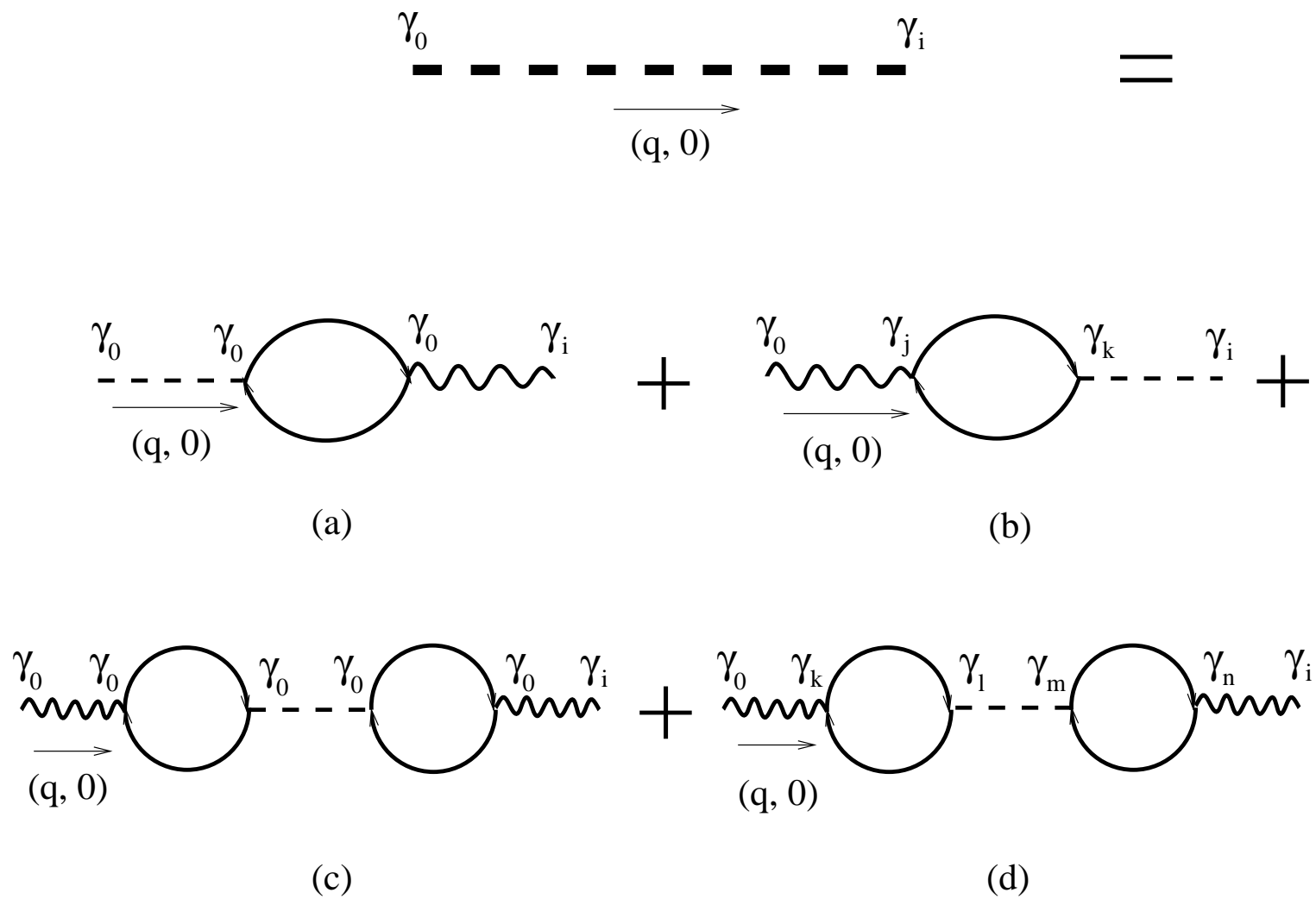


Fig.3

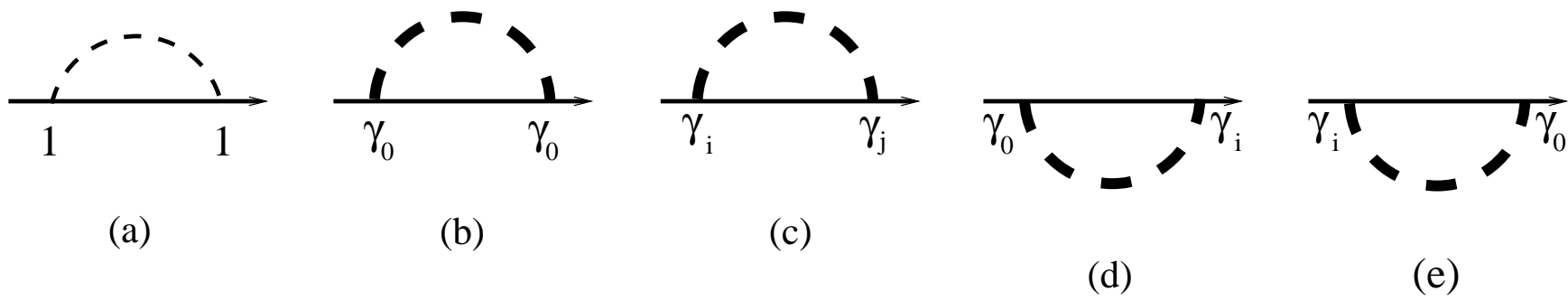


Fig.4

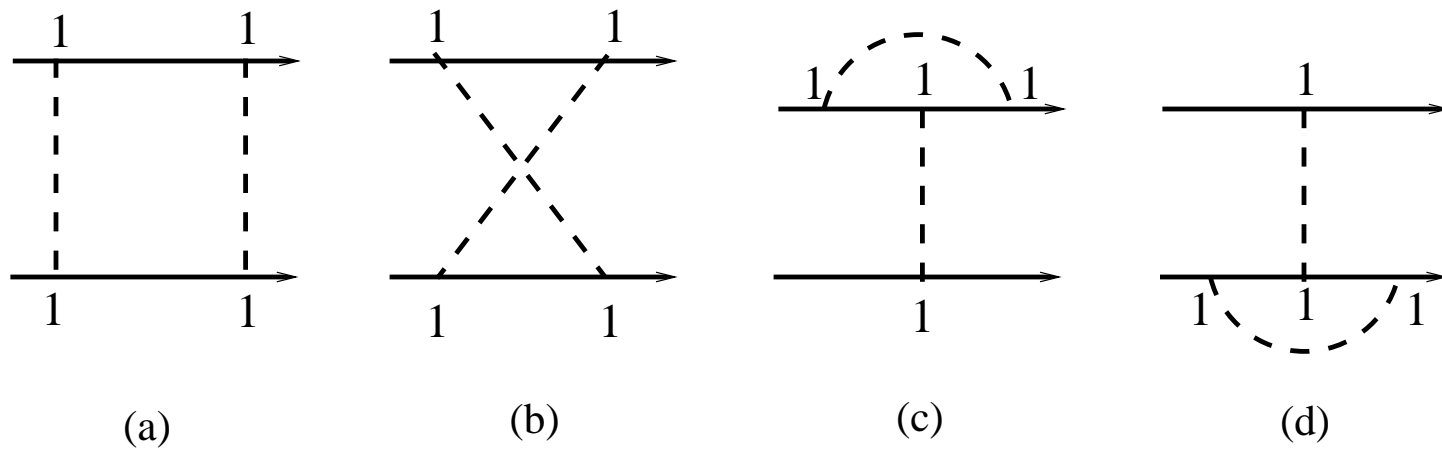


Fig.5

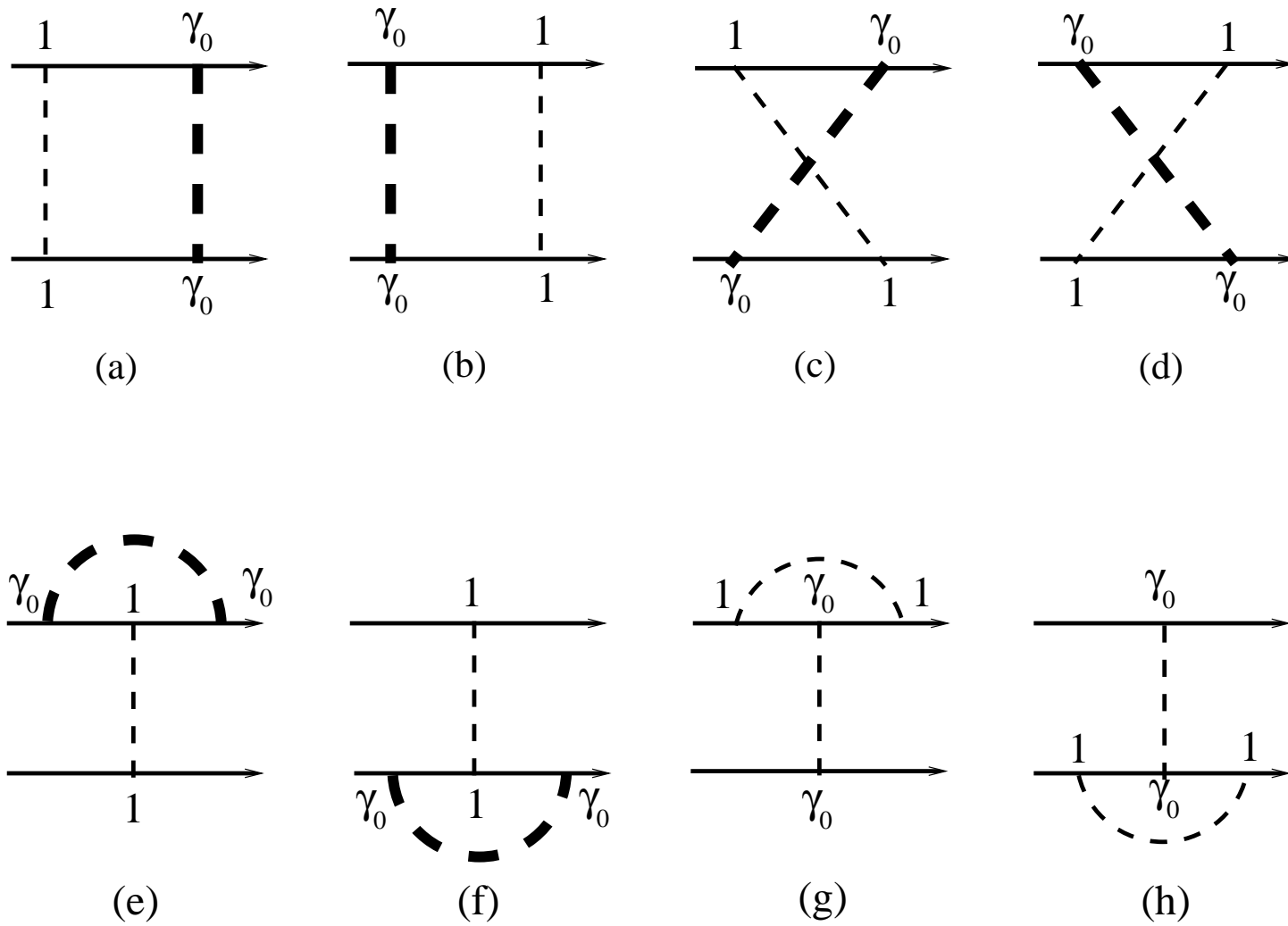


Fig.6

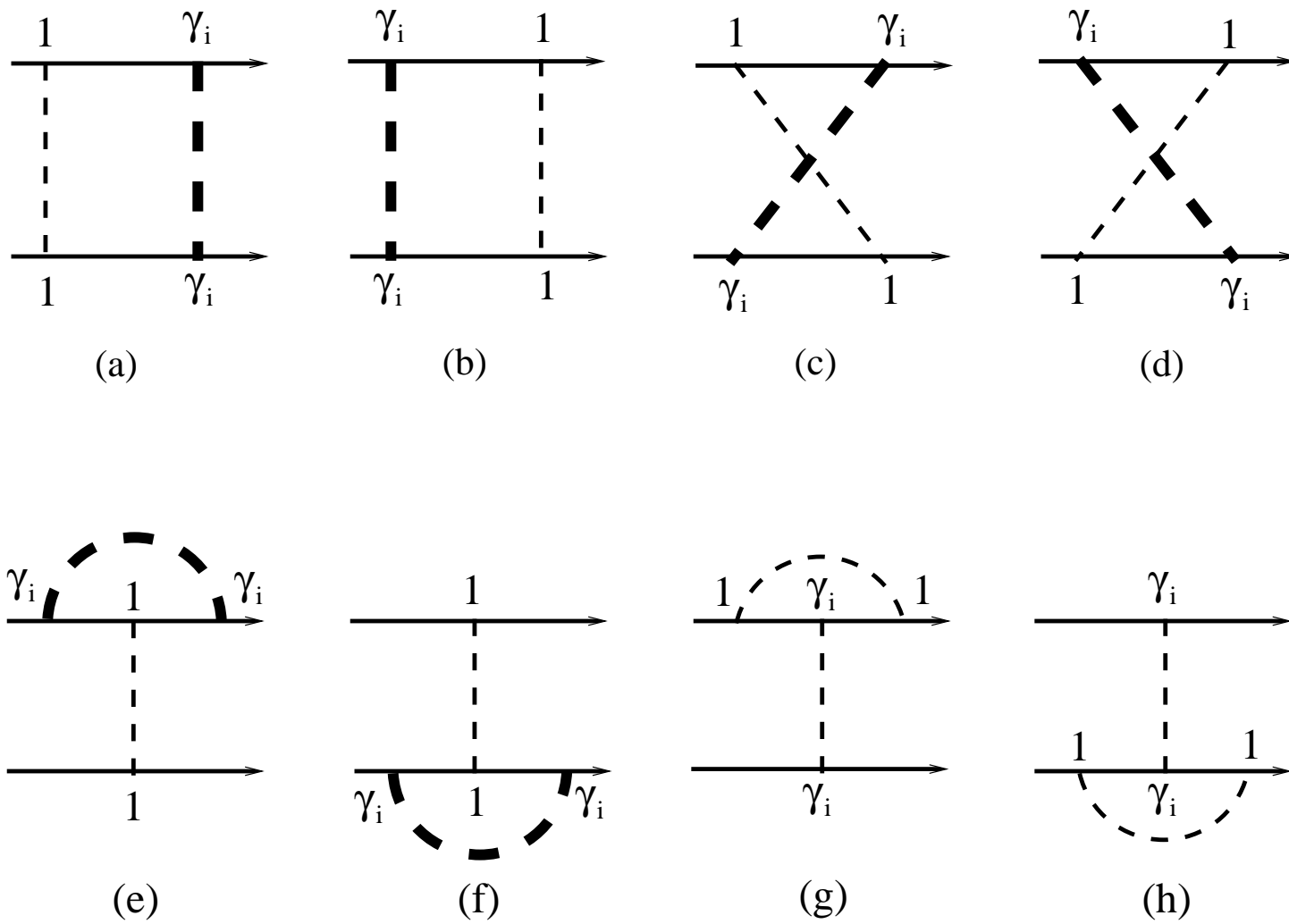


Fig.7

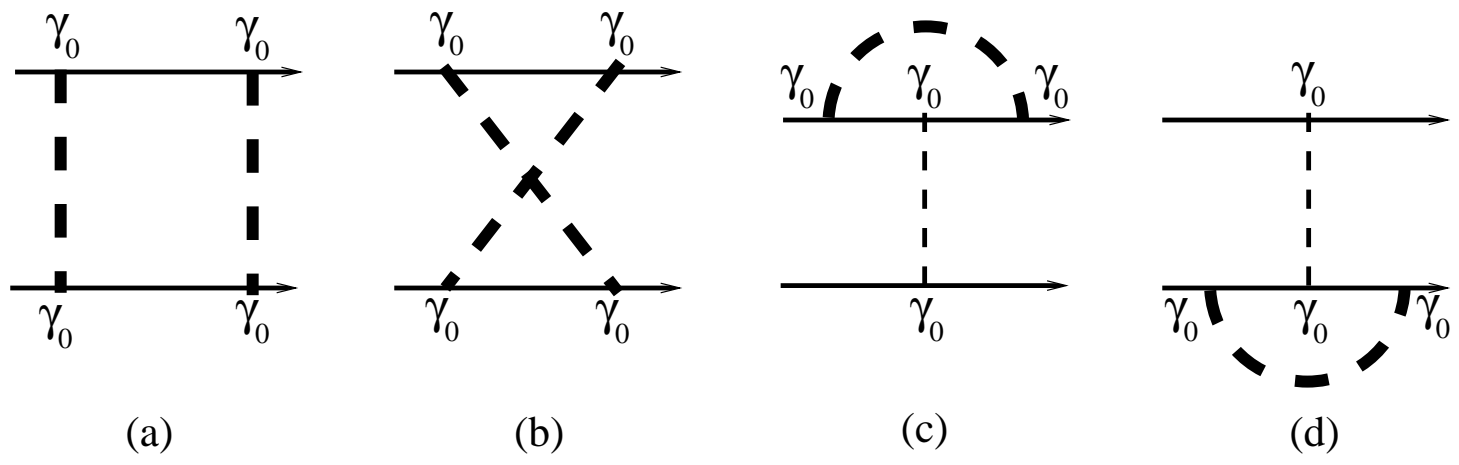


Fig.8

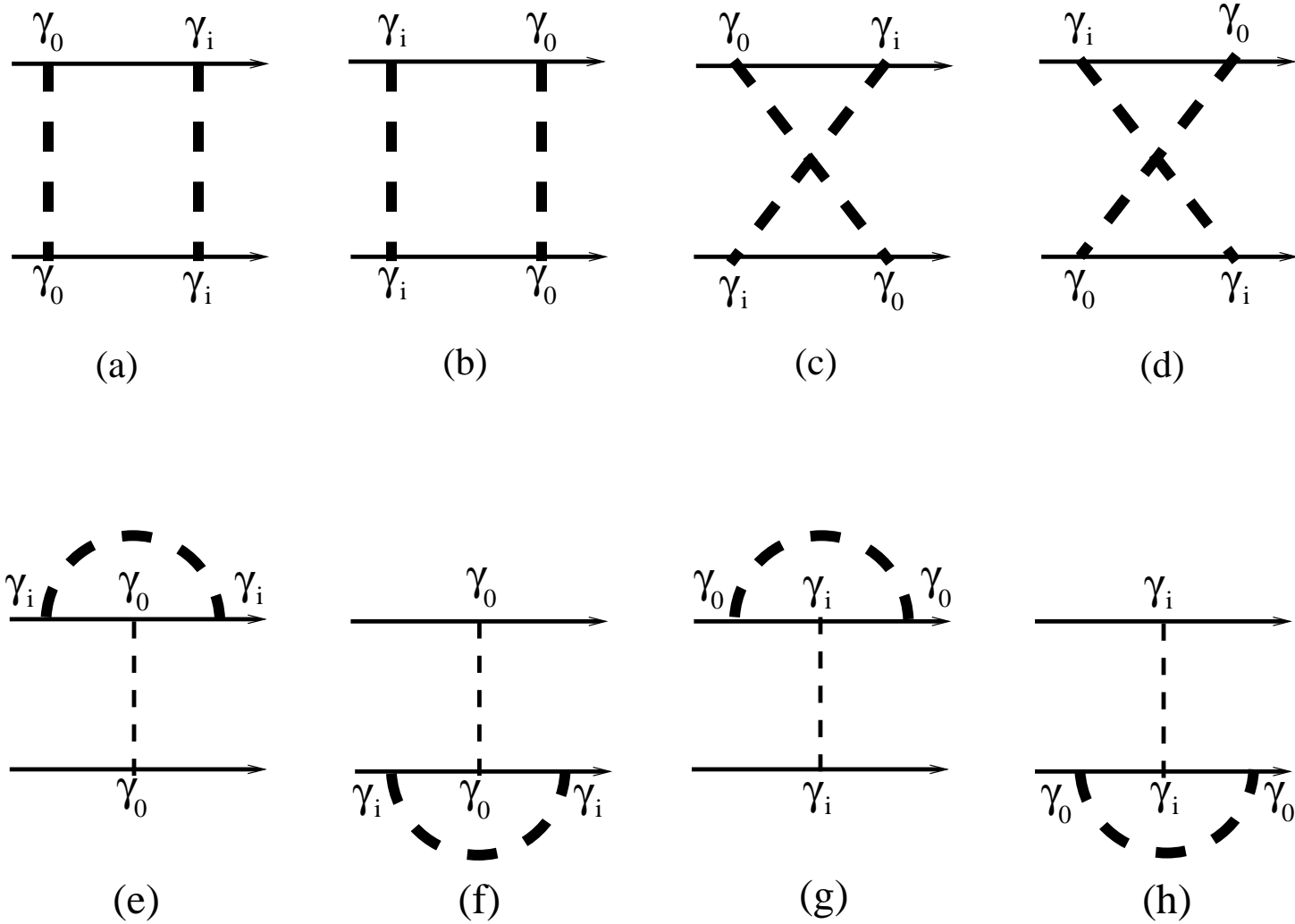


Fig.9

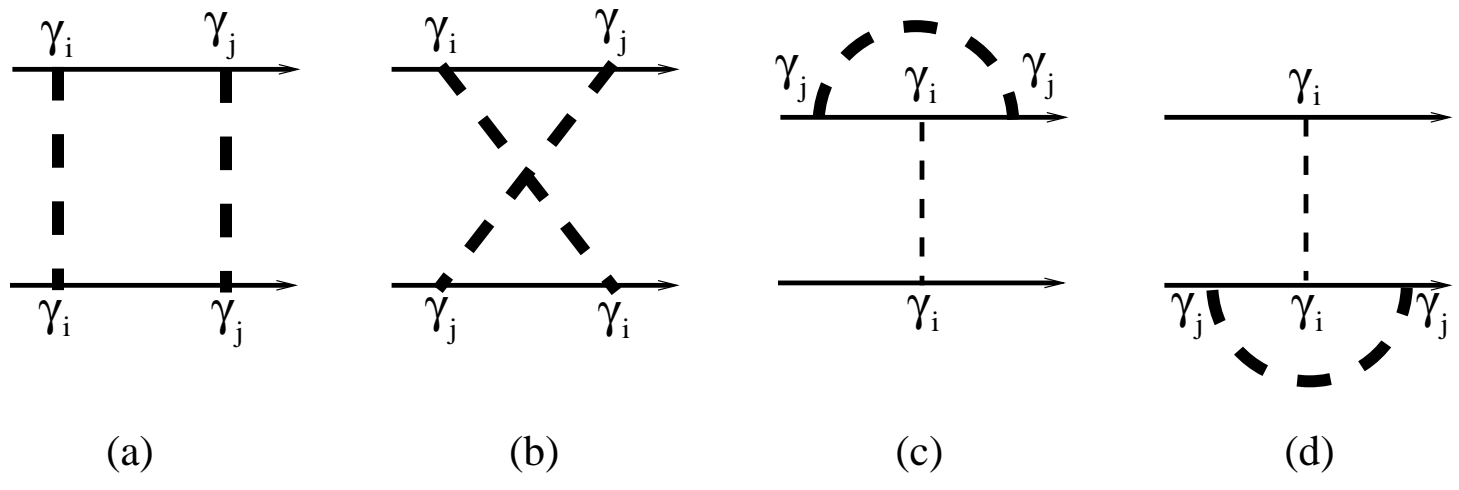


Fig.10

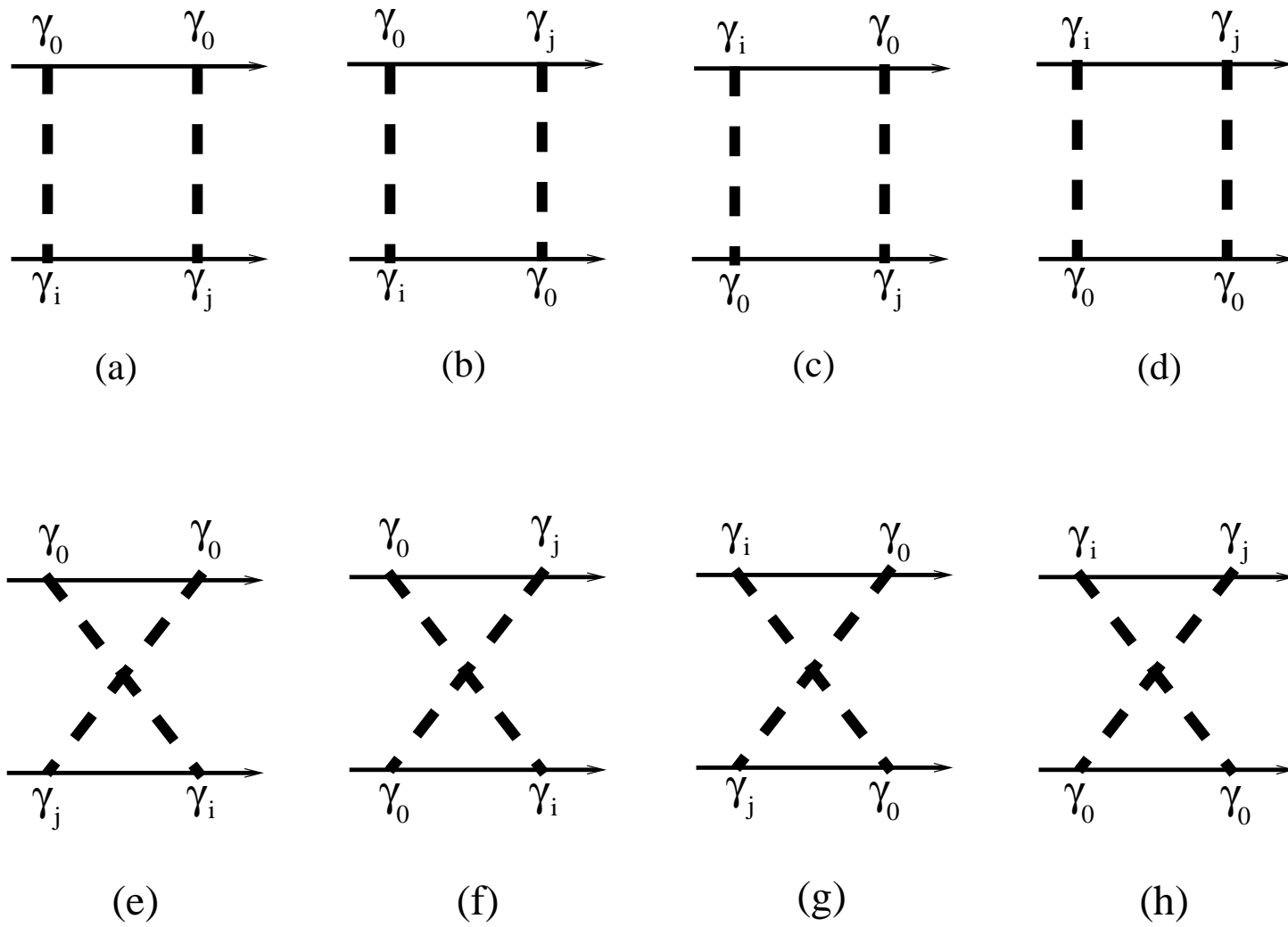


Fig.11

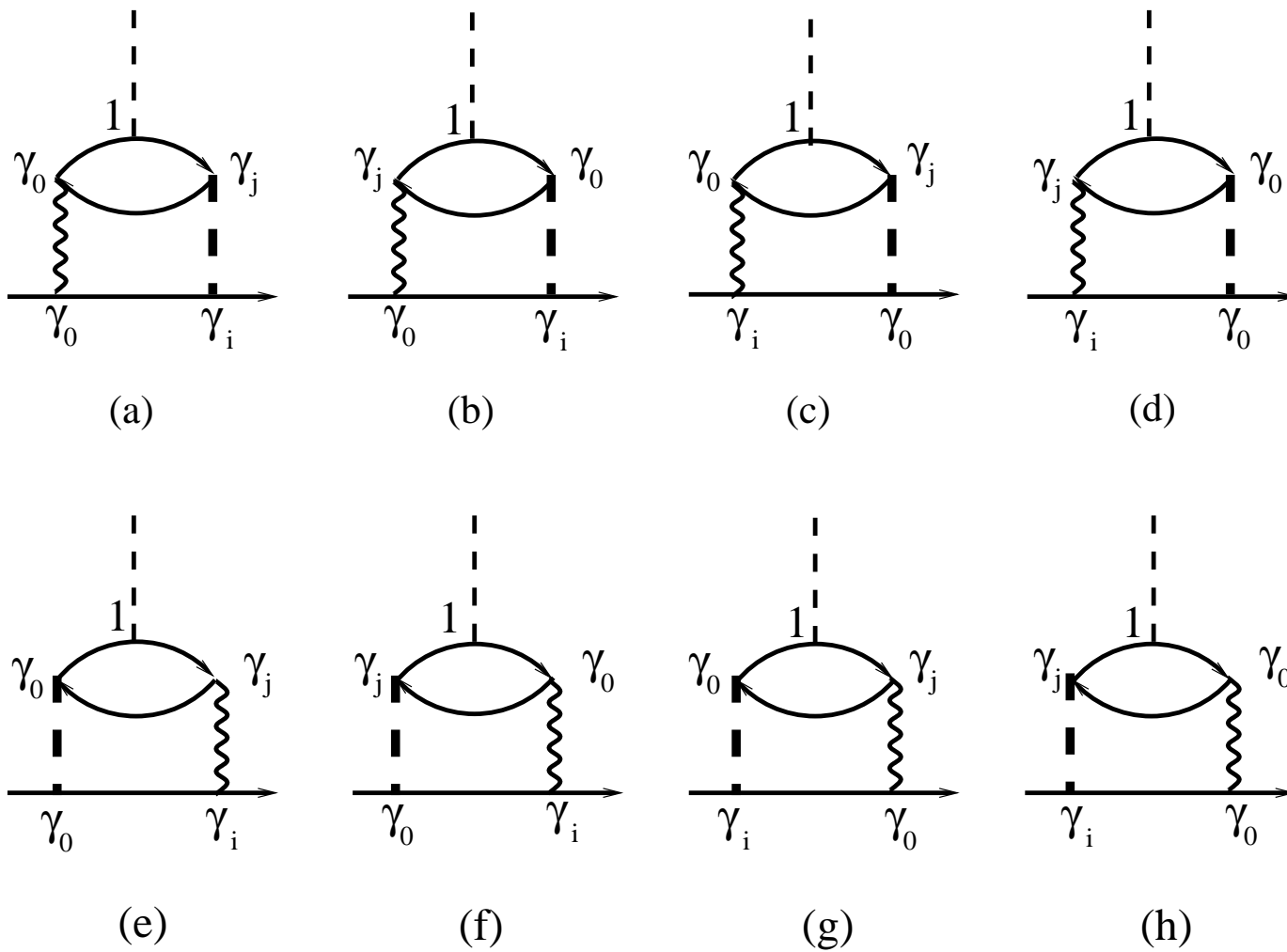


Fig.12

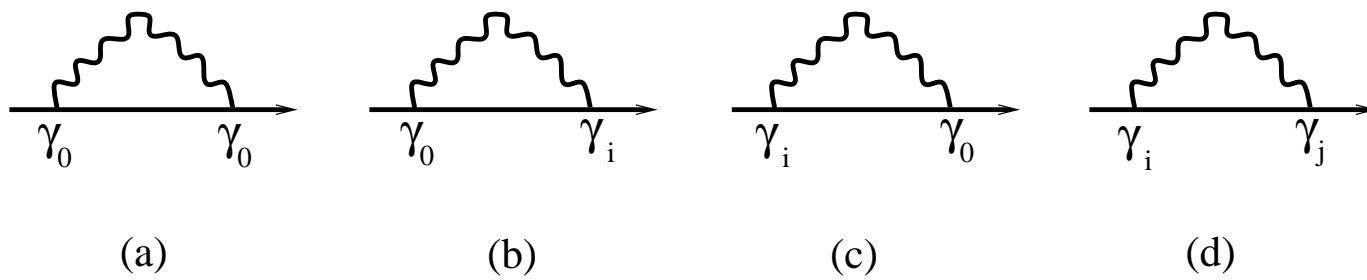


Fig.13

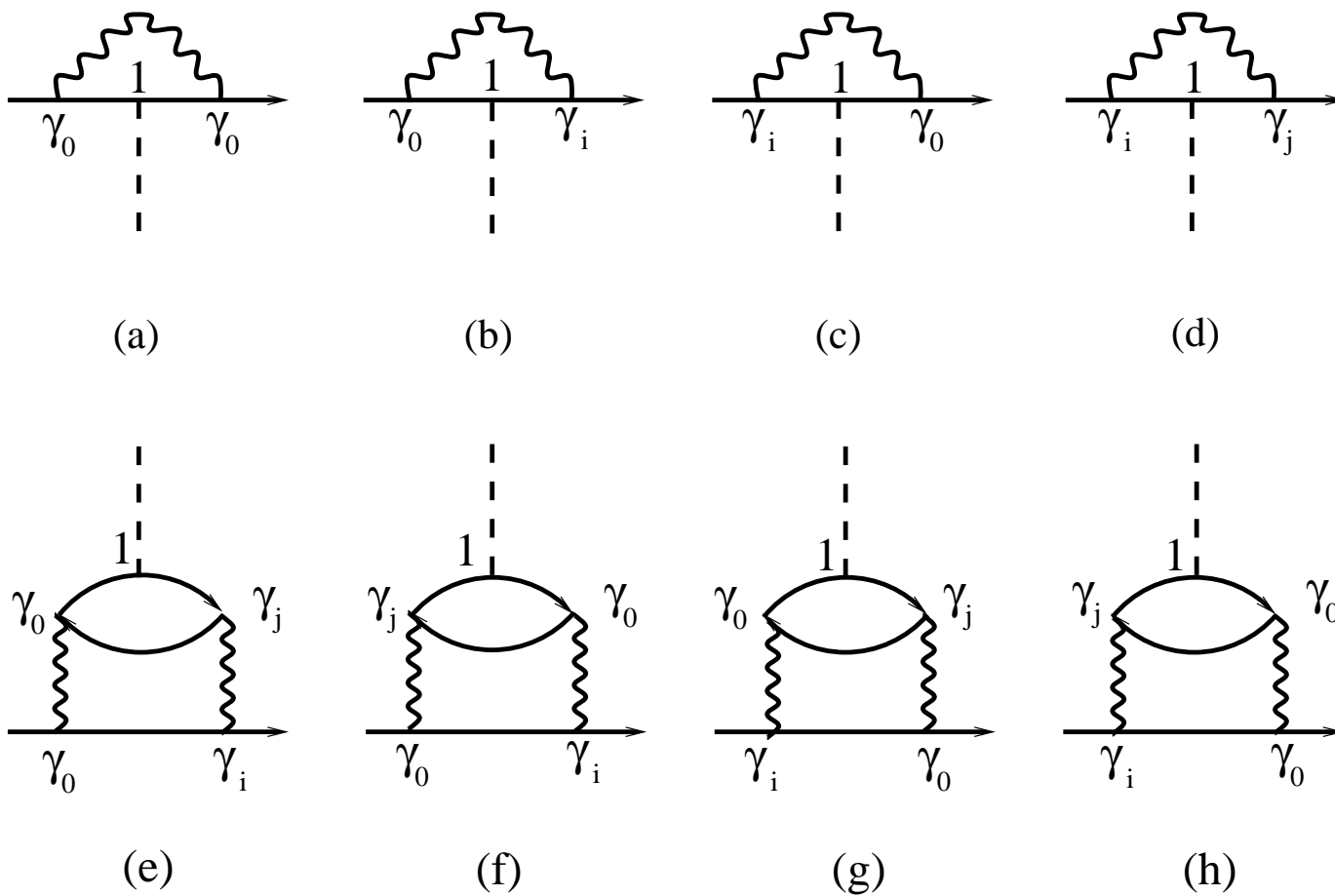


Fig.14

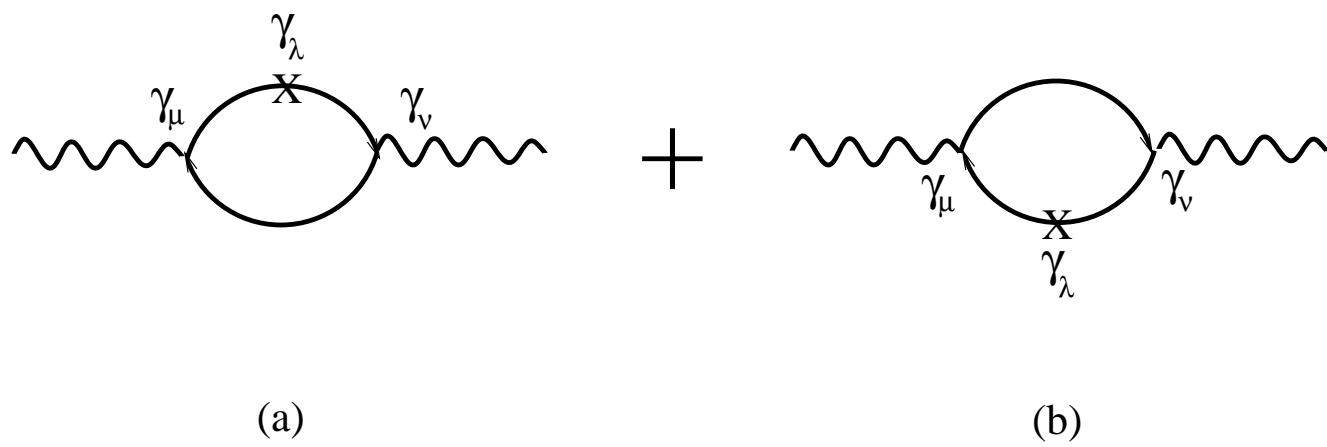
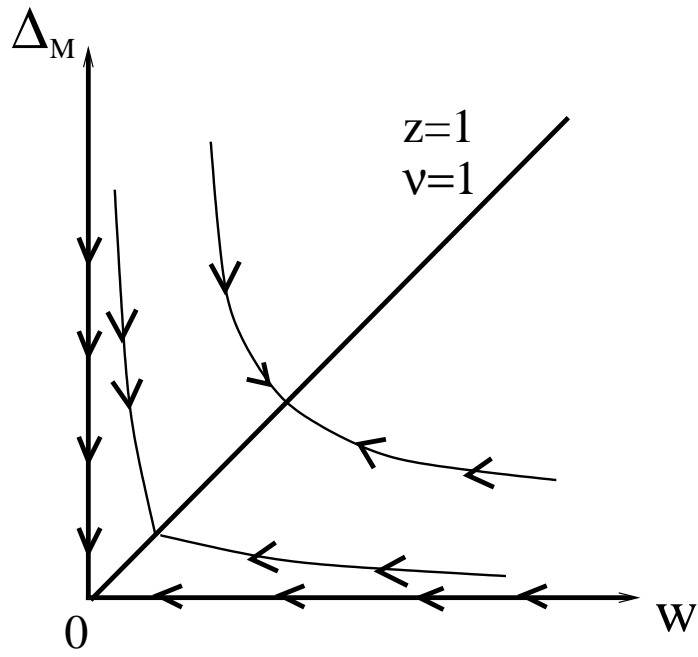
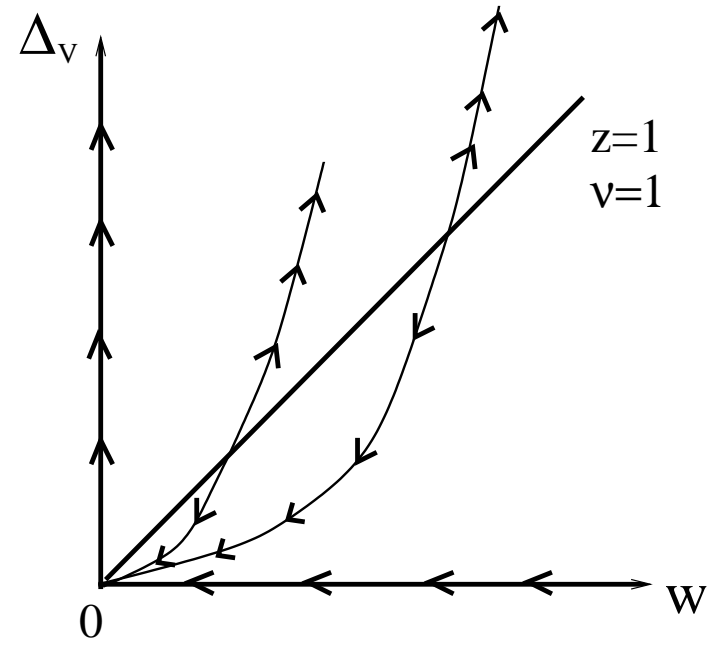


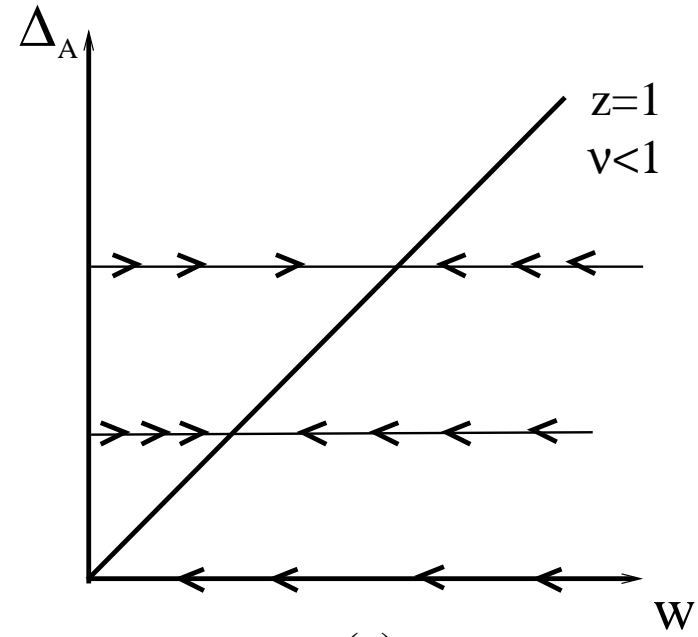
Fig.15



(a)

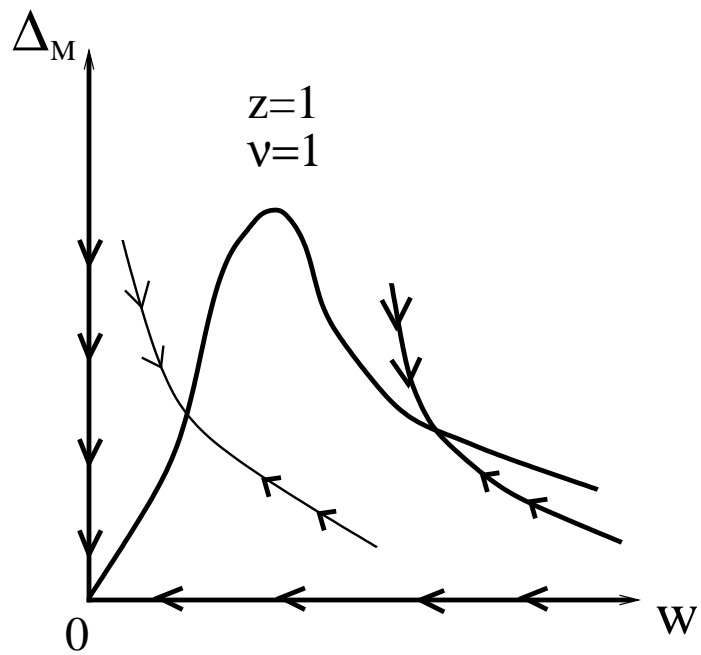


(b)

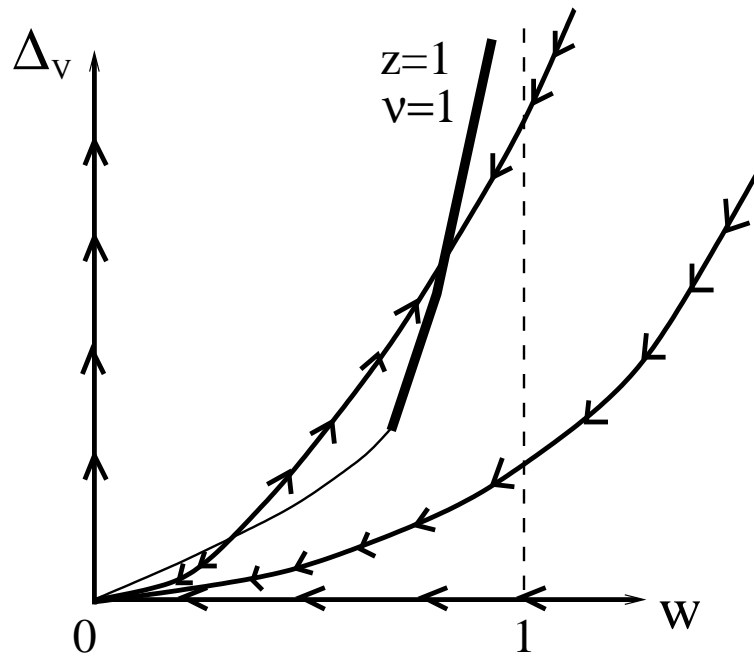


(c)

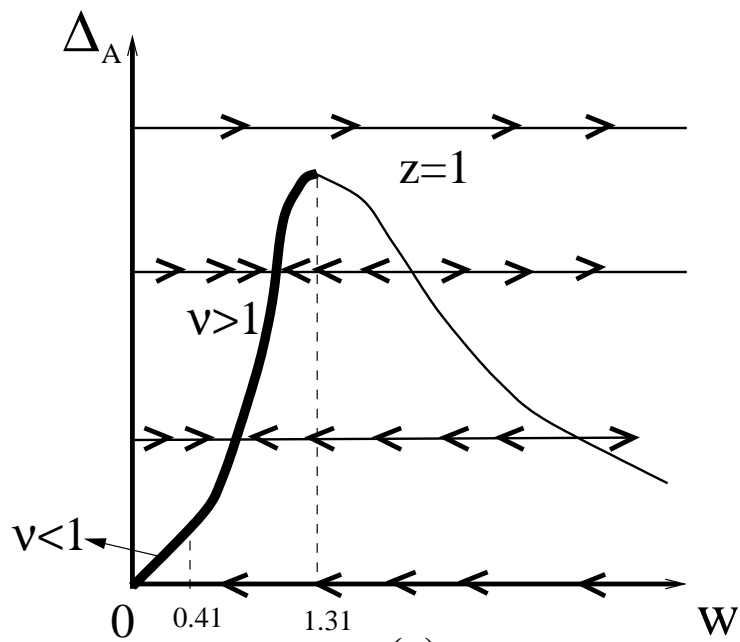
Fig.16



(a)



(b)



(c)

Fig.17

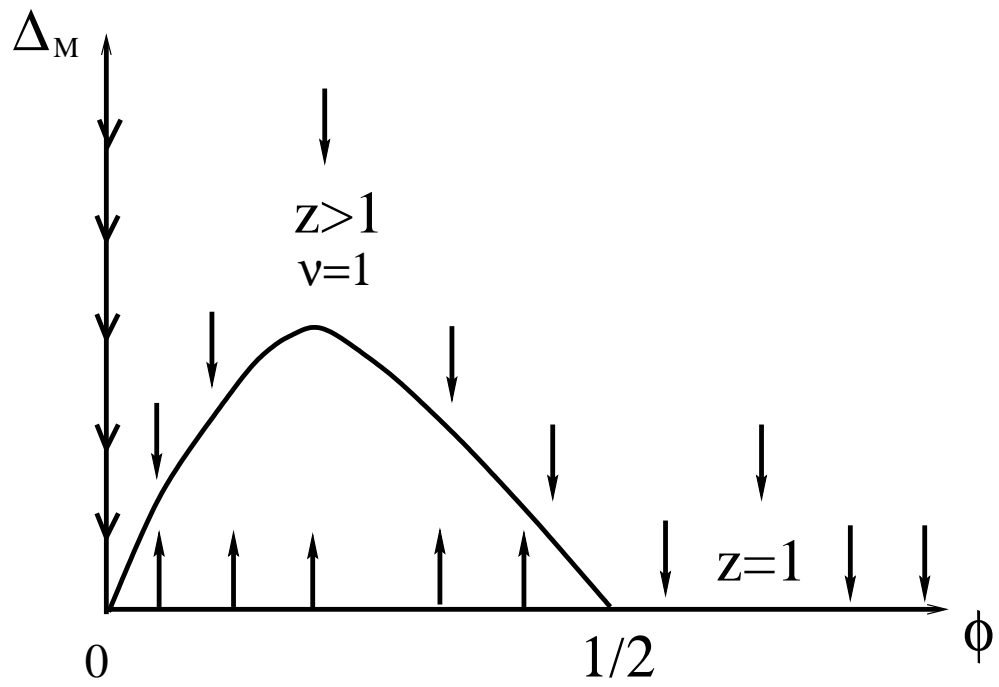


Fig.18

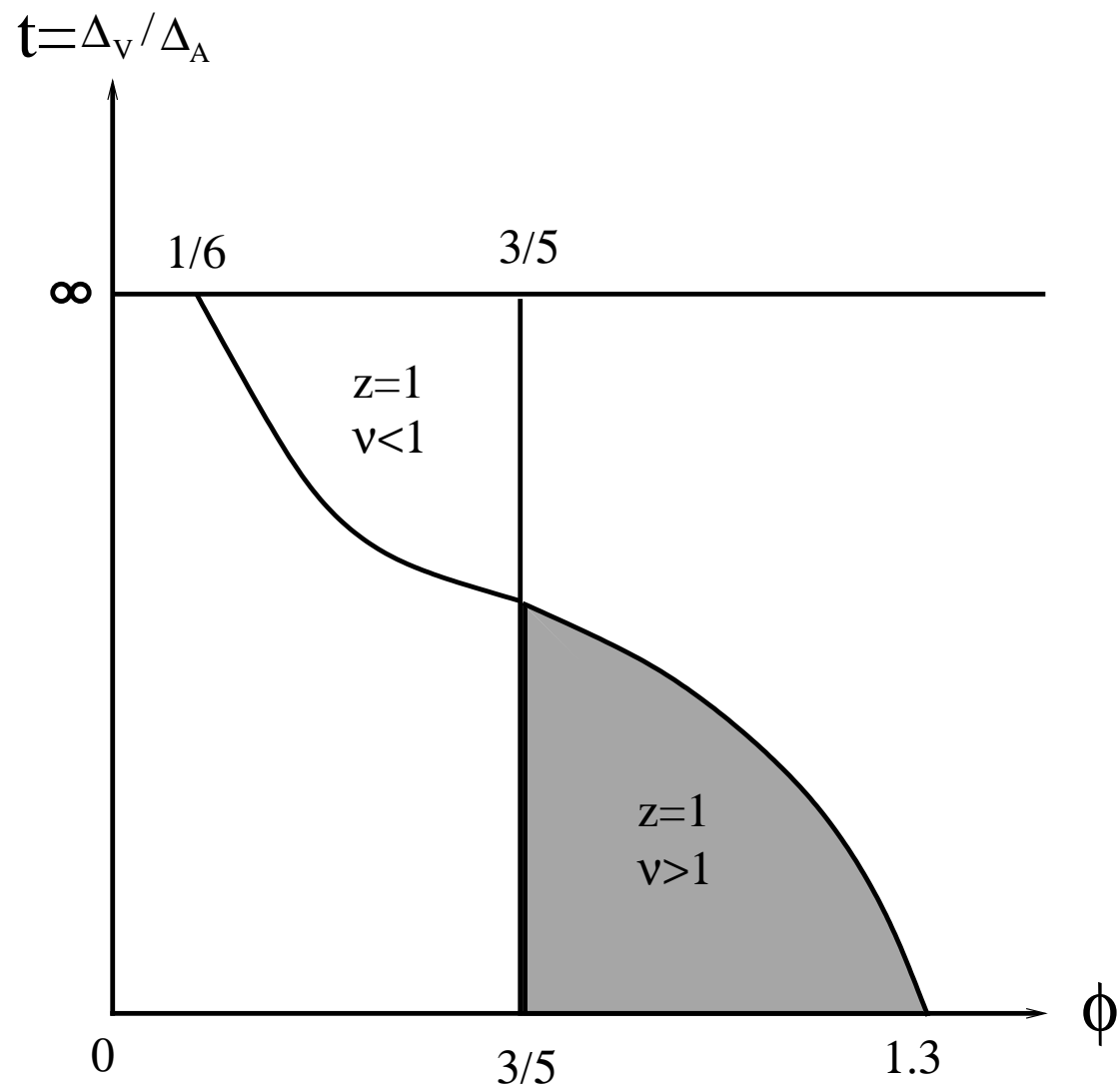


Fig.19